Angewandte Chemie
Eine Zeitschrift der Gesellschaft Deutscher Chemiker

Supporting Information

Discrete Stacked Dimers of Aromatic Oligoamide Helices

*D. Bindl, P. K. Mandal, L. Allmendinger, I. Huc**

Contents

List of Abbreviations

AcOH	acetic acid
CD	circular dichroism
CyHex	cyclohexane
DCM	dichloromethane
DIPEA	*N*,*N*-diisopropylethylamine
DMF	*N*,*N*-dimethylformamide
DMSO	dimethyl sulfoxide
EI	electron ionization
ESI	electrospray ionization
EtOAc	ethyl acetate
Fmoc	fluorenylmethoxycarbonyl
HMBC	heteronuclear multiple bond correlation
HMQC	heteronuclear multiple quantum correlation
HSQC	heteronuclear single quantum correlation
HPLC	high performance liquid chromatography
HRMS	high resolution mass spectrometry
MeOH	methanol
MW	molecular weight
NMR	nuclear magnetic resonance
RP	reversed phase
RT	room temperature
SPFS	solid phase foldamer synthesis
TEA	triethylamine
THF	tetrahydrofuran
TLC	thin layer chromatography
TMSP	3-(trimethylsilyl)propionic-2,2,3,3-d_4 acid sodium salt
UV/Vis	ultraviolet-visible

1 Supplementary figures

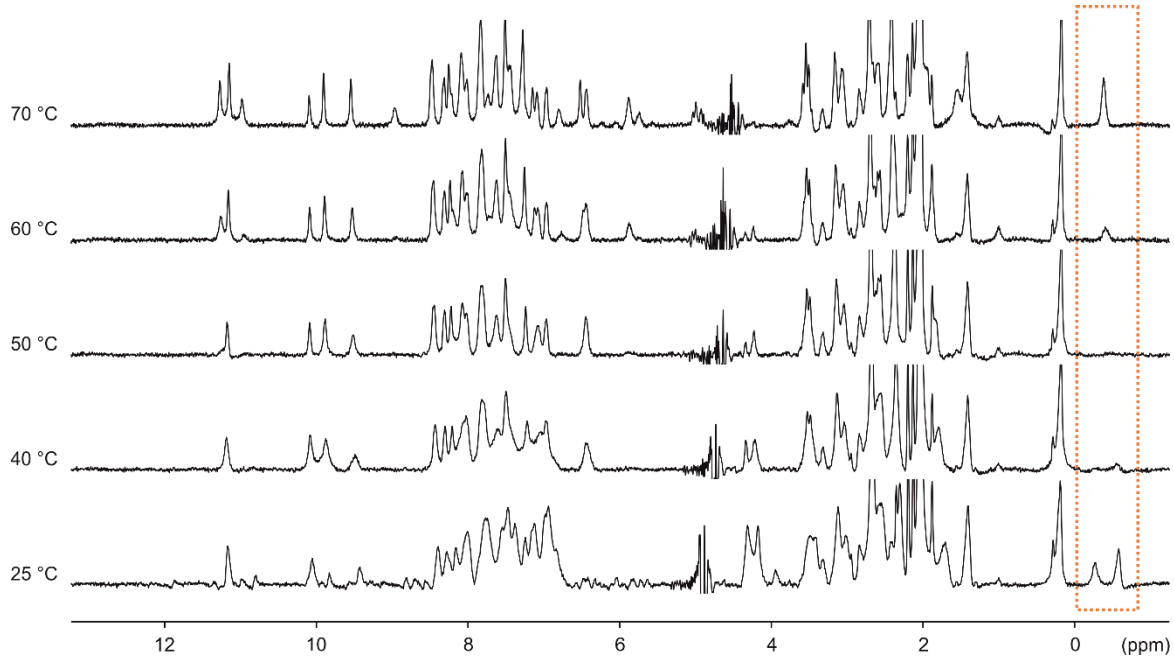

Figure S1. Variable temperature ^{1}H NMR of compound **1** (400 MHz, 0.35 mM in 12 mM ammonium acetate aqueous buffer pH 8.5). Coalescence is observed at 50 °C for the chiral methyl group of the B^{Rme} unit (below 0 ppm).

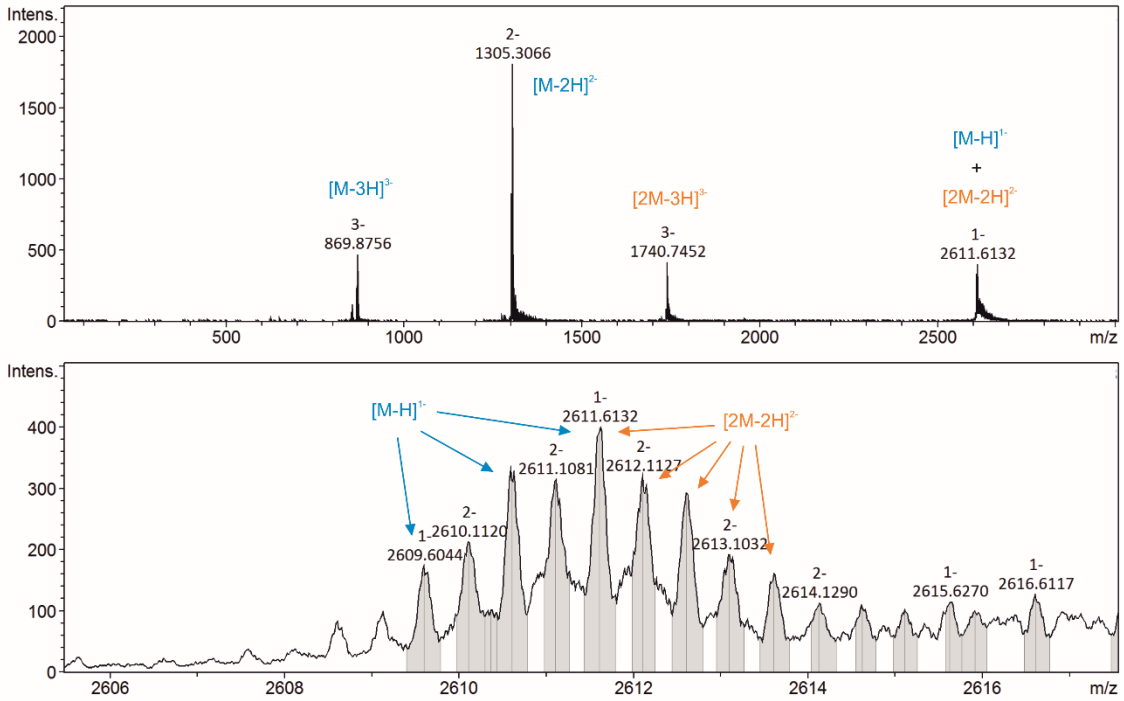

Figure S2. ESI-MS spectrum of compound **1** (direct infusion of an aqueous sample). Peaks originating from monomeric and dimeric species are highlighted in blue and orange, respectively. The $[M-H]^{1-}$ peak is superimposed by the $[2M-2H]^{2-}$ peak, while the mass envelope suggests a major population of the $[2M-2H]^{2-}$ species.

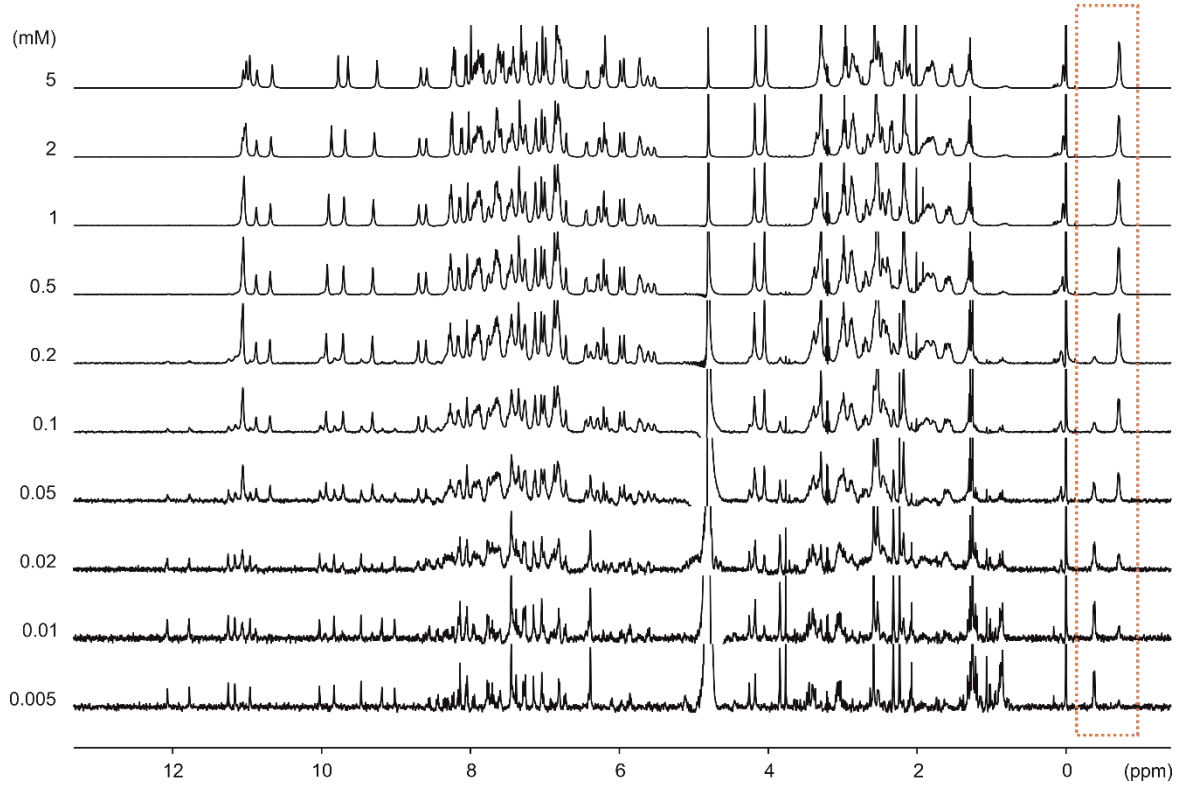

Figure S3. Variable concentration ^{1}H NMR spectra of compound **1** (500 MHz, 27 mM sodium phosphate aqueous buffer pH 7.0). Concentrations of **1** are shown next to the respective spectrum, buffer concentrations were kept constant. Integrals used for binding curve plotting are marked in orange.

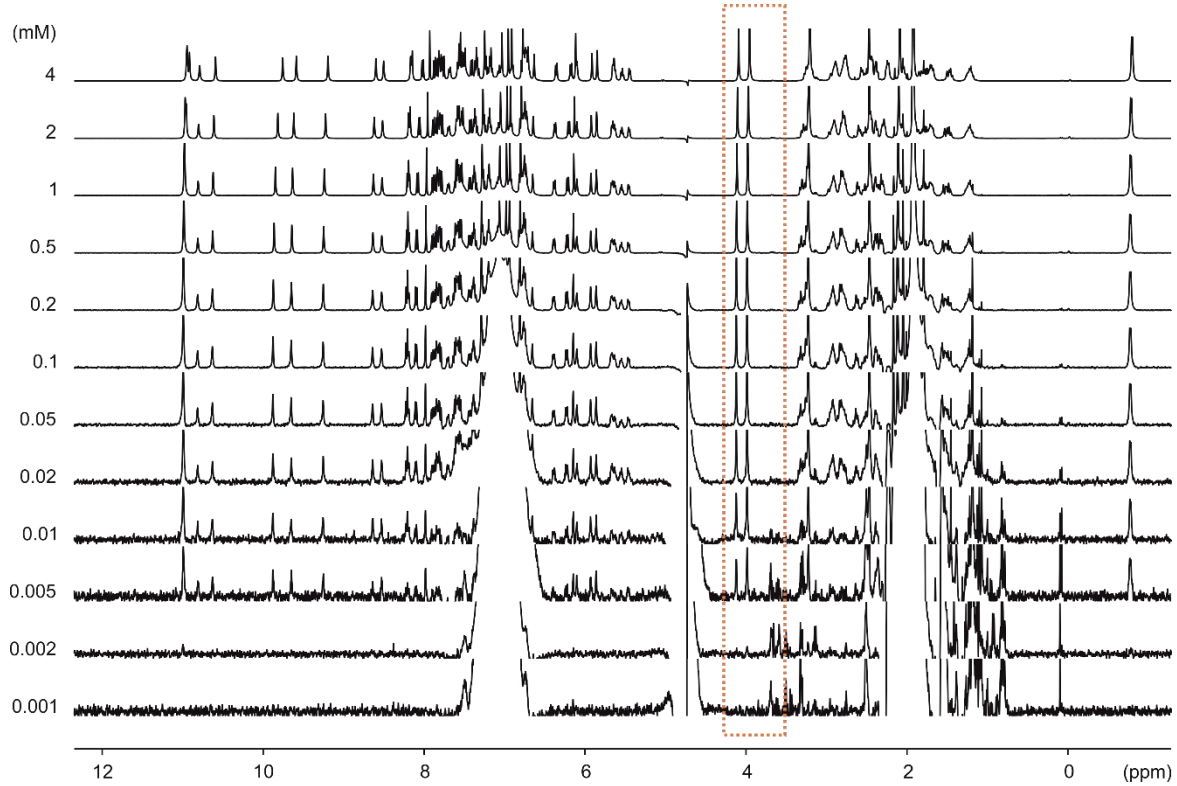

Figure S4. Variable concentration ^{1}H NMR spectra of compound **1** (500 MHz, 14 mM ammonium acetate aqueous buffer pH 5.0). Concentrations of **1** are shown next to the respective spectrum, buffer concentrations were kept constant. Integrals used for binding curve plotting are marked in orange.

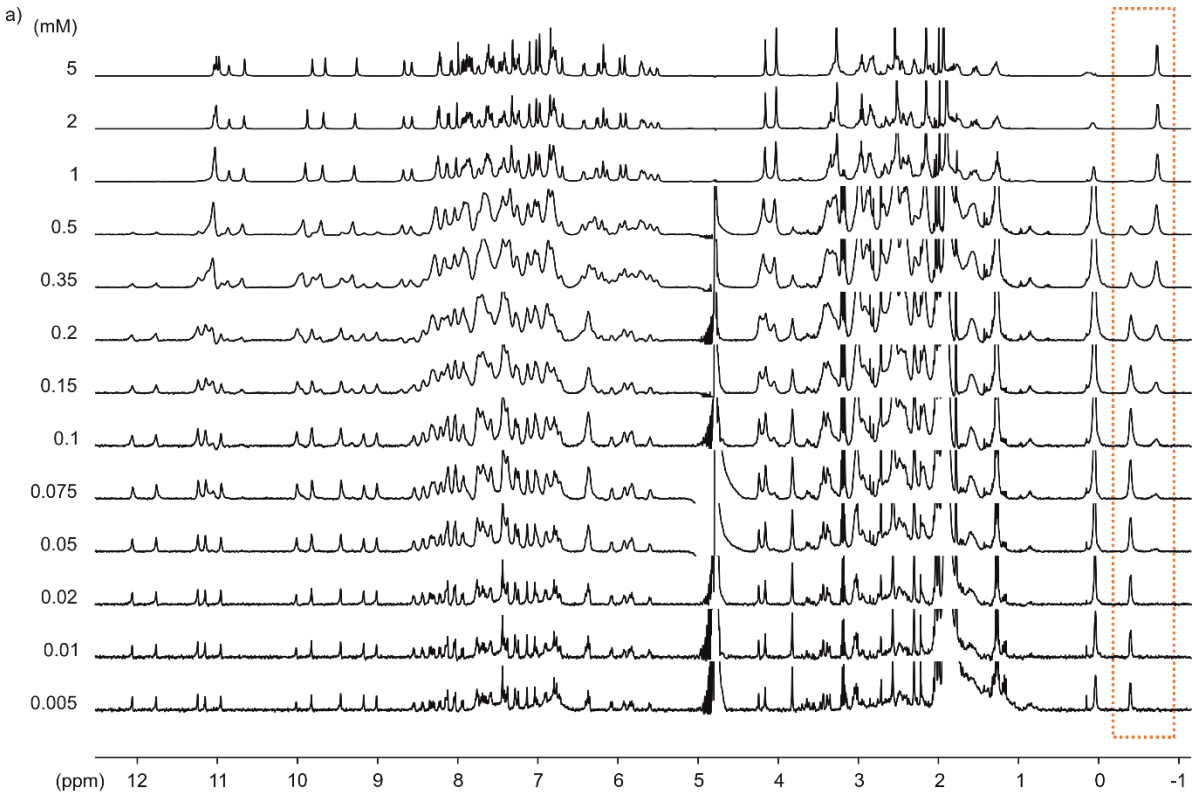

b) pH 7.0

c (mM)	Integral
5	100%
2	99%
1	98%
0.5	96%
0.2	87%
0.1	75%
0.05	61%
0.02	34%
0.01	23%
0.005	10%

5.0

c (mM)	Integral
4	100%
2	100%
1	100%
0.5	100%
0.2	100%
0.1	100%
0.05	100%
0.02	97%
0.01	95%
0.005	76%
0.002	15%
0.001	8%

8.5

c (mM)	Integral
5	100%
2	100%
1	95%
0.5	75%
0.35	64%
0.2	41%
0.15	35%
0.1	19%
0.075	15%
0.05	11%
0.02	0%
0.01	0%
0.005	0%

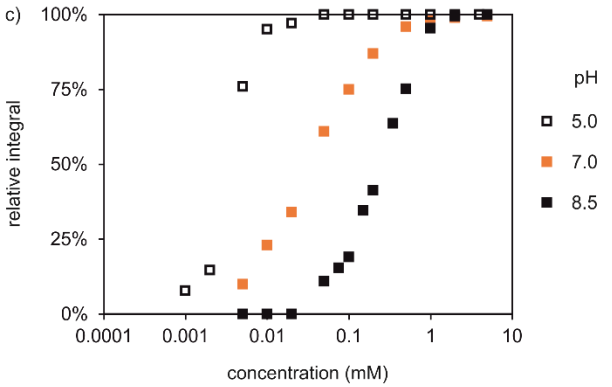

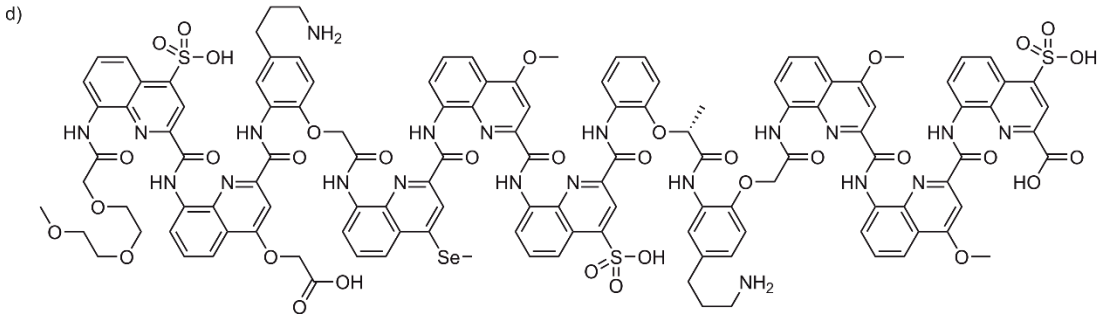

Figure S5. a) Variable concentration ^{1}H NMR spectra of compound **1** (500 MHz, 12 mM ammonium acetate aqueous buffer pH 8.5). Concentrations of **1** are shown next to the respective spectrum, buffer concentrations were kept constant. Integrals used for binding curve plotting are marked in orange. Data (b) and plot (c) of the relative integrals of the aggregated compared to the monomeric species. d) Chemical structure of compound **1**.

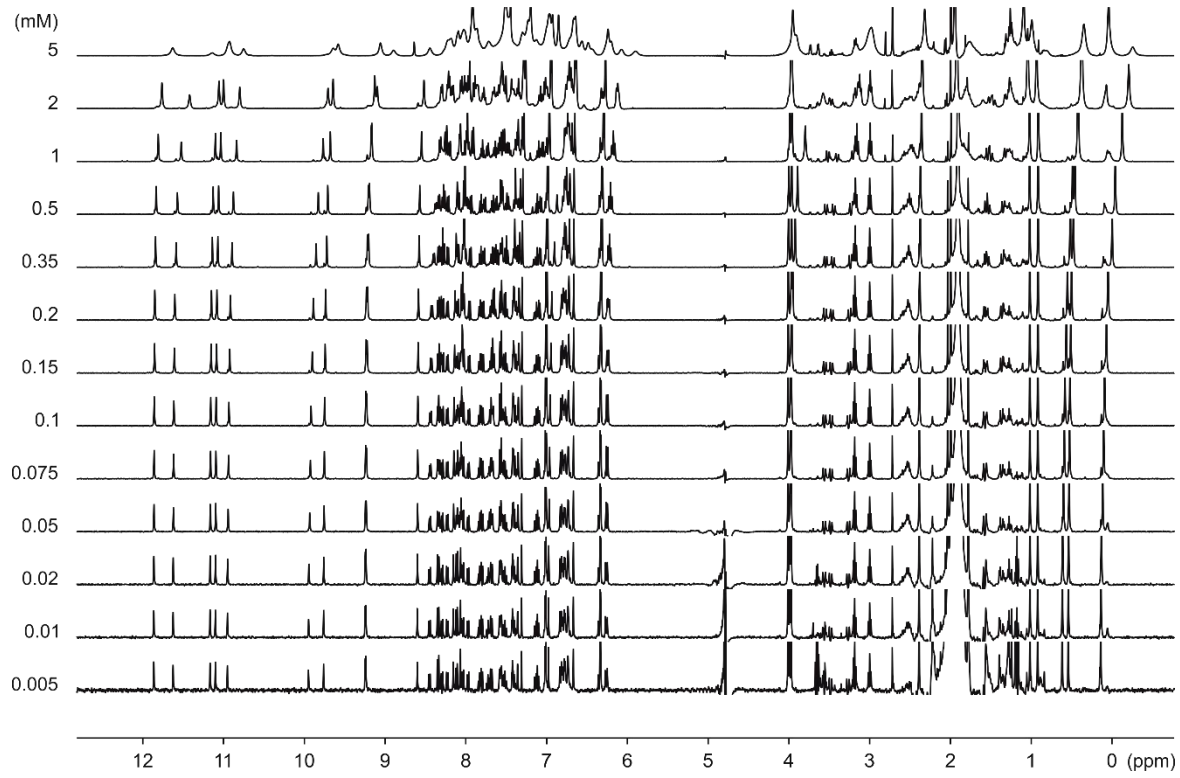

Figure S6. Variable concentration ^{1}H NMR spectra of compound **2** (500 MHz, 12 mM ammonium acetate aqueous buffer pH 8.5). Concentrations of **2** are shown next to the respective spectrum, buffer concentrations were kept constant.

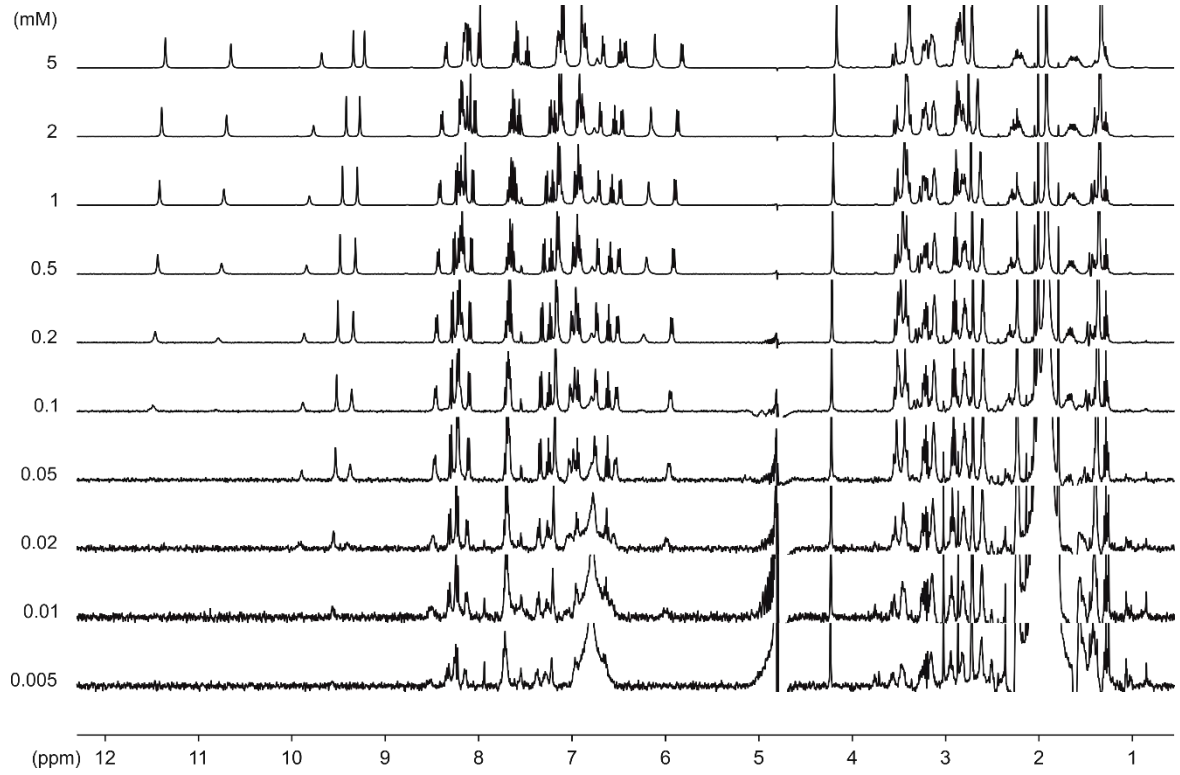

Figure S7. Variable concentration ^{1}H NMR spectra of compound **5** (500 MHz, 12 mM ammonium acetate aqueous buffer pH 8.5). Concentrations of **5** are shown next to the respective spectrum, buffer concentrations were kept constant.

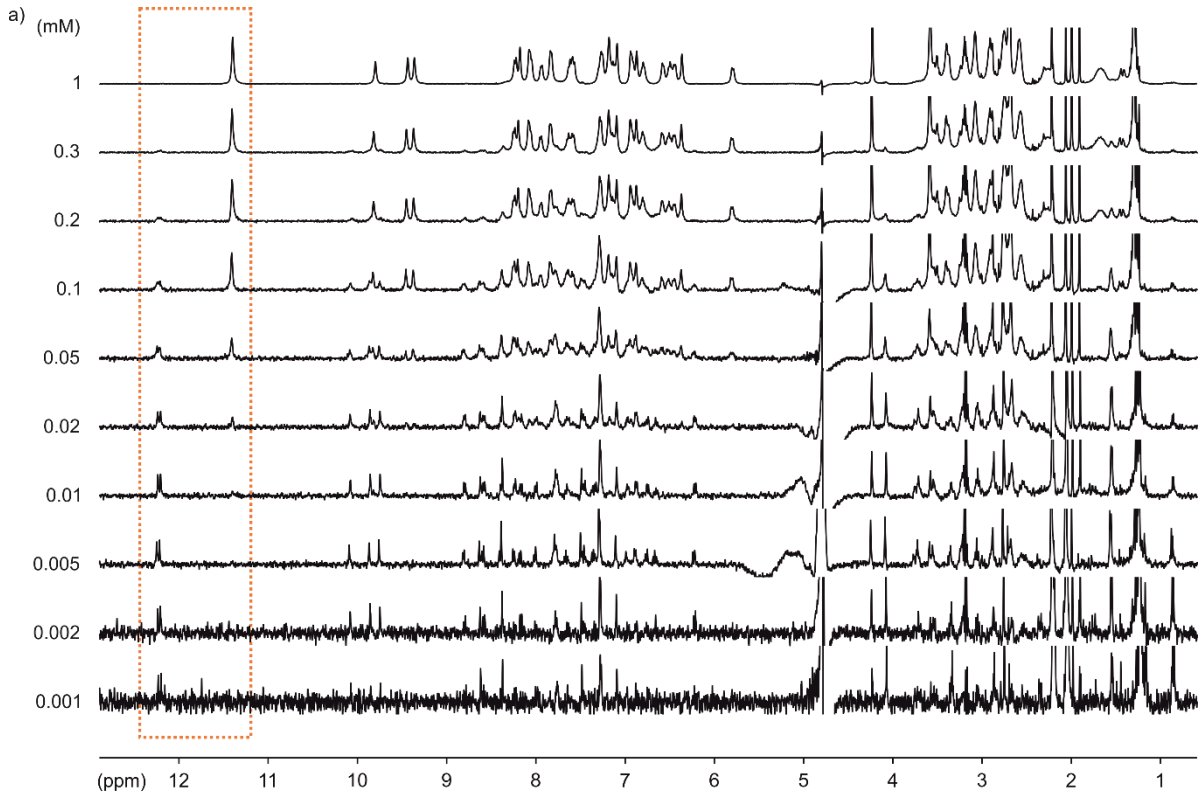

b)

c (mM)	Integral
1	100%
0.3	94%
0.2	87%
0.1	71%
0.05	54%
0.02	29%
0.01	16%
0.005	7%
0.002	0%
0.001	0%

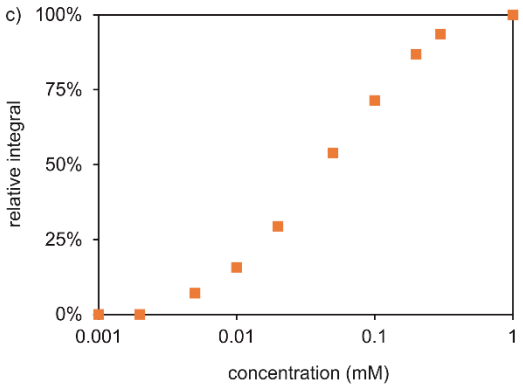

d)

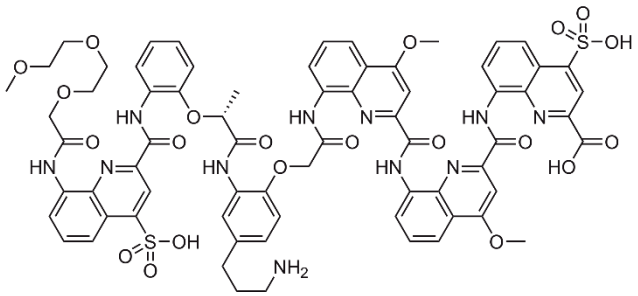

Figure S8. a) Variable concentration ^{1}H NMR spectra of compound **4** (500 MHz, 27 mM sodium phosphate aqueous buffer pH 7.0). Concentrations of **4** are shown next to the respective spectrum, buffer concentrations were kept constant. Integrals used for binding curve plotting are marked in orange. Data (b) and plot (c) of the relative integrals of the aggregated compared to the monomeric species. d) Chemical structure of compound **4**.

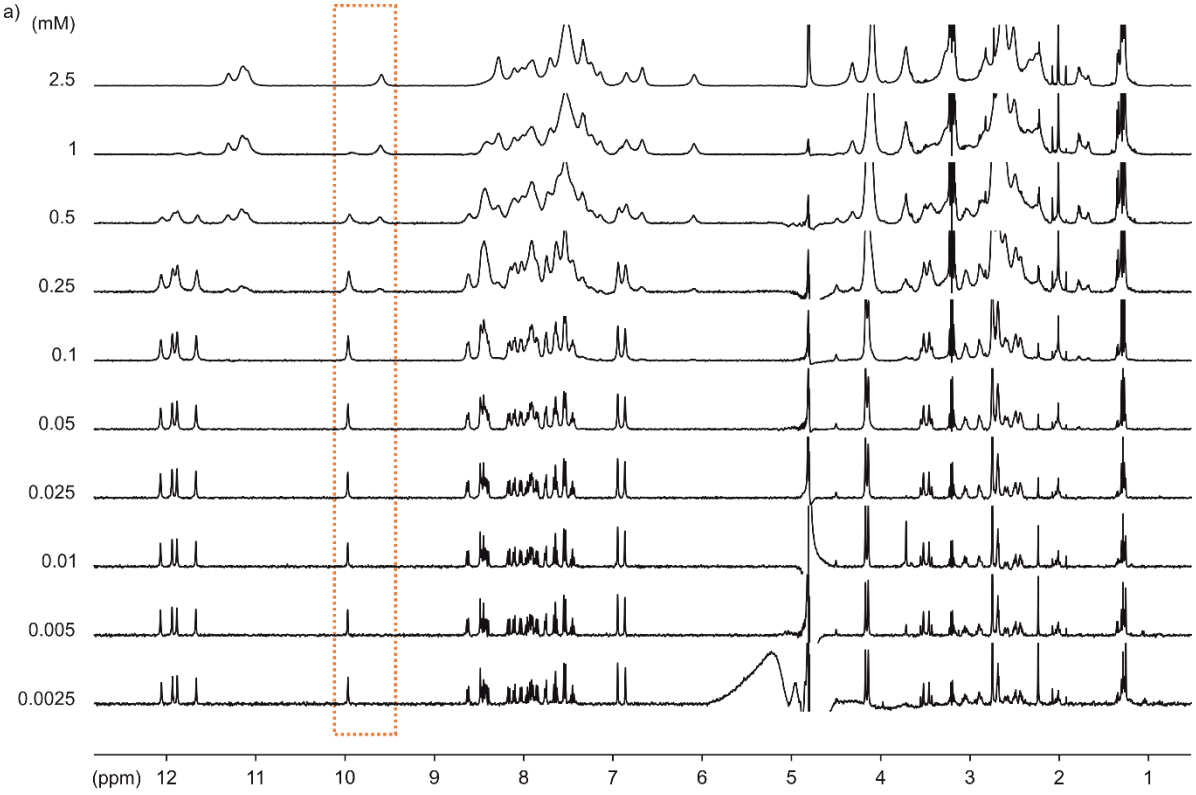

b)

c (mM)	Integral
2.5	100%
1	83%
0.5	43%
0.25	17%
0.1	8%
0.05	0%
0.025	0%
0.01	0%
0.005	0%
0.0025	0%

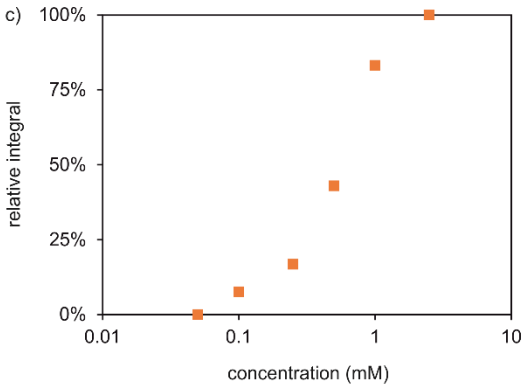

d)

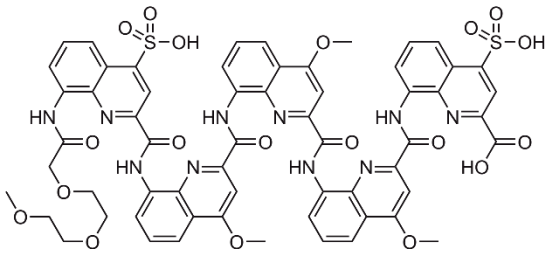

Figure S9. a) Variable concentration ^{1}H NMR spectra of compound **6** (500 MHz, 27 mM sodium phosphate aqueous buffer pH 7.0). Concentrations of *P*-**6**/*M*-**6** (total concentration has been divided by two, since only homomeric dimerization is possible) are shown next to the respective spectrum, buffer concentrations were kept constant. Integrals used for binding curve plotting are marked in orange. Data (b) and plot (c) of the relative integrals of the aggregated compared to the monomeric species. d) Chemical structure of compound **6**.

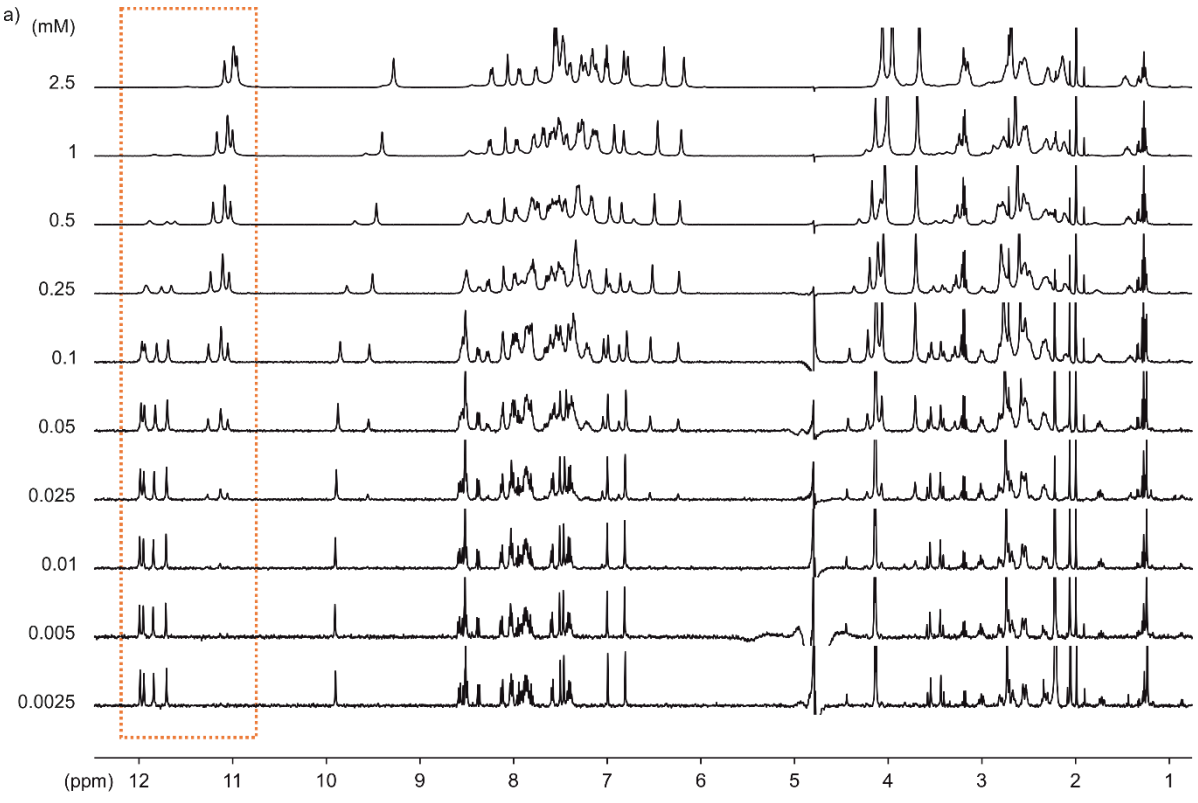

b)

c (mM)	Integral
2.5	98%
1	92%
0.5	84%
0.25	72%
0.1	47%
0.05	31%
0.025	20%
0.01	7%
0.005	1%
0.0025	0%

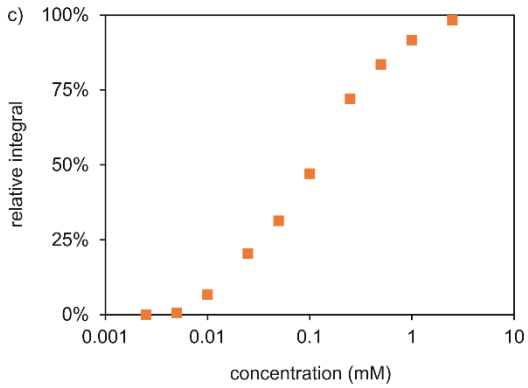

d)

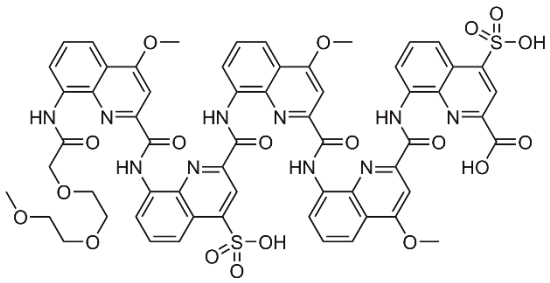

Figure S10. a) Variable concentration ^{1}H NMR spectra of compound **7** (500 MHz, 27 mM sodium phosphate aqueous buffer pH 7.0). Concentrations of *P*-**7**/*M*-**7** (total concentration has been divided by two, since only homomeric dimerization is possible) are shown next to the respective spectrum, buffer concentrations were kept constant. Integrals used for binding curve plotting are marked in orange. Data (b) and plot (c) of the relative integrals of the aggregated compared to the monomeric species. d) Chemical structure of compound **7**.

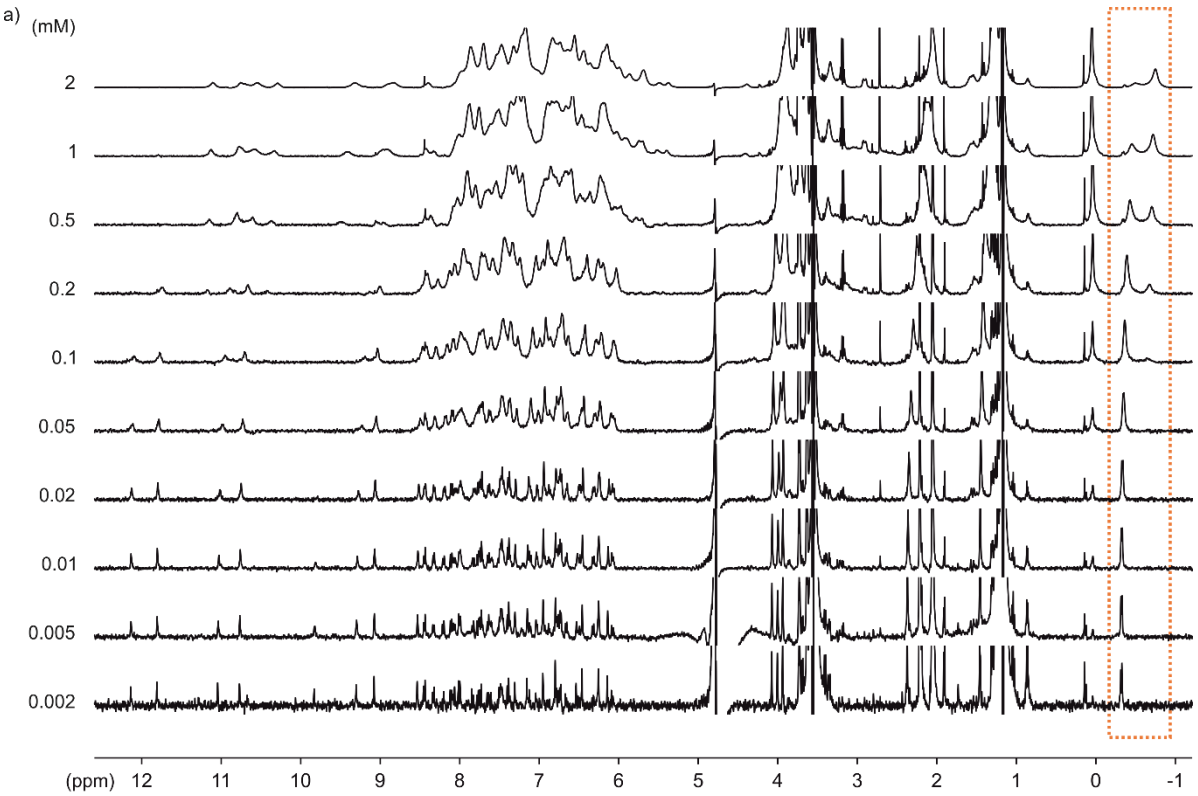

b)

c (mM)	Integral
2	77%
1	63%
0.5	46%
0.2	24%
0.1	16%
0.05	2%
0.02	0%
0.01	0%
0.005	0%
0.002	0%

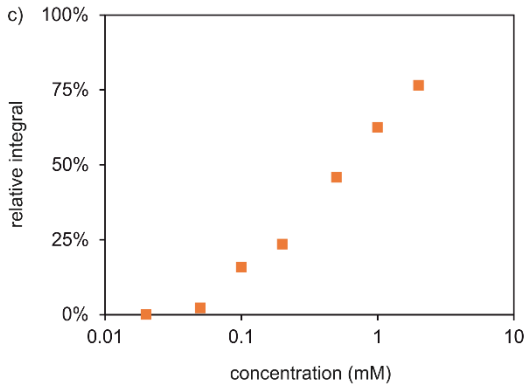

d)

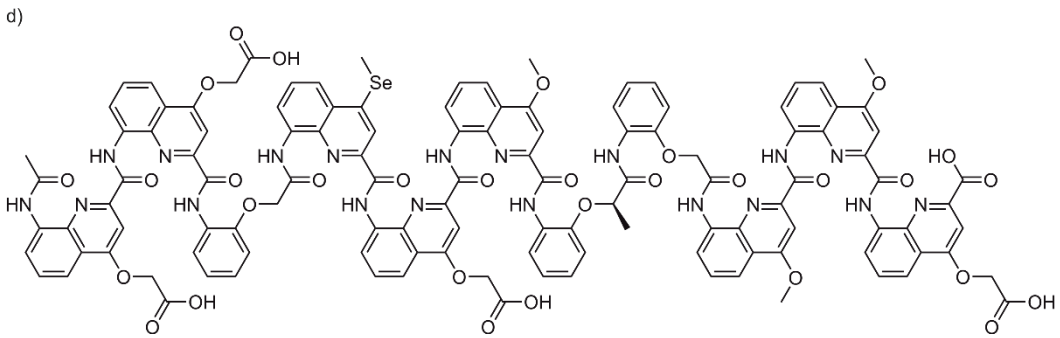

Figure S11. a) Variable concentration ^{1}H NMR spectra of compound **8** (500 MHz, 27 mM sodium phosphate aqueous buffer pH 7.0). Concentrations of **8** are shown next to the respective spectrum, buffer concentrations were kept constant. Integrals used for binding curve plotting are marked in orange. Data (b) and plot (c) of the relative integrals of the aggregated compared to the monomeric species. d) Chemical structure of compound **8**.

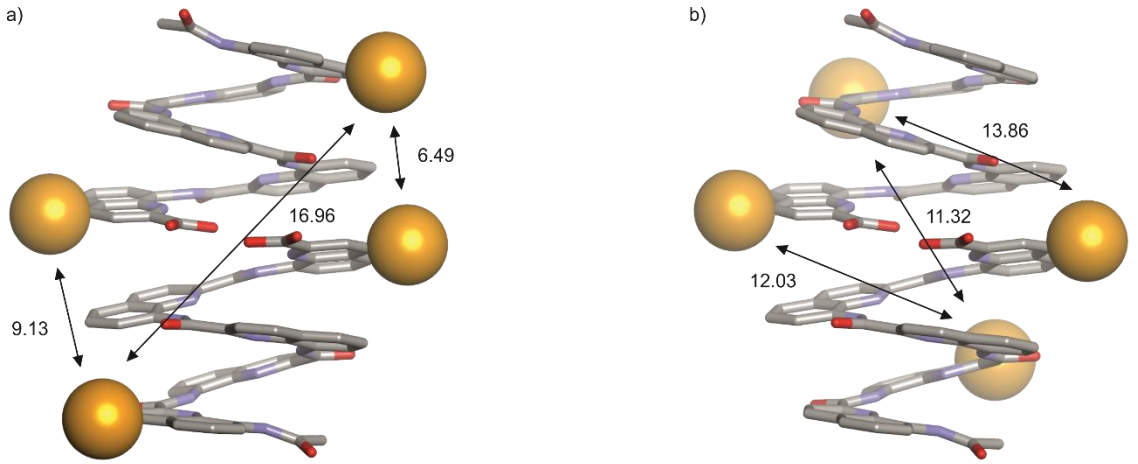

Figure S12. Models of compounds **6** (a) and **7** (b) (Energy minimized using Maestro, Method: TNCG, Forcefield: OPLS3, Solvent: water). Hydrogen atoms and side chains are omitted for clarity. The sulfur atoms of the Q^{Sul} units are shown as yellow balls. Intermolecular distances between sulfur atoms (except between the C-terminal Q^{Sul} units) is depicted in Angstrom (Å). Compound **6** shows shorter distances (>10 Å) compared to **7**.

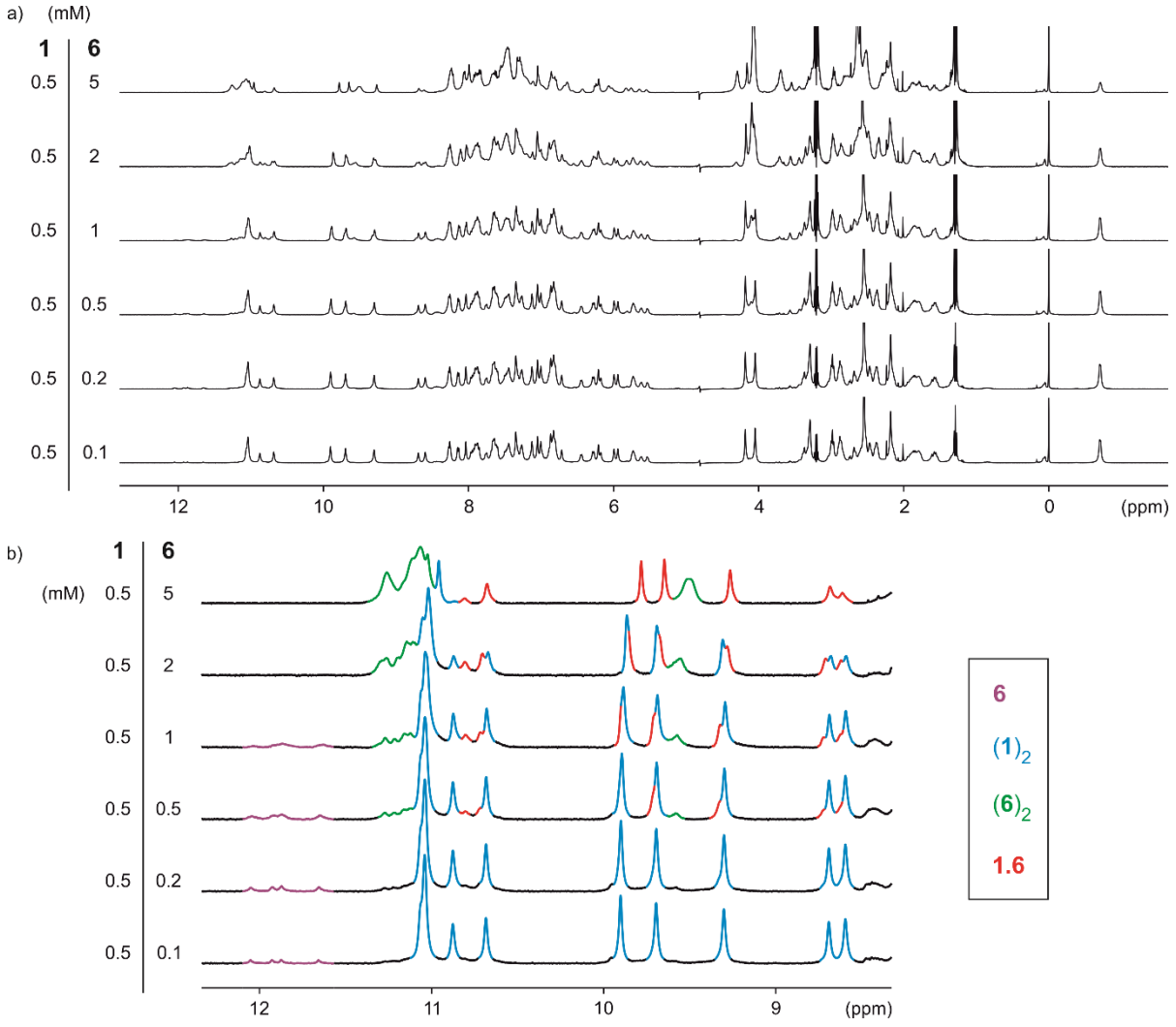

Figure S13. Variable concentration ^{1}H NMR spectra of mixtures of compound **1** and **6** (500 MHz, 27 mM sodium phosphate aqueous buffer pH 7.0). Concentrations of **1** and **6** are shown next to the respective spectrum, buffer concentrations were kept constant. a) Full spectra without coloration. b) Zoom on the amide region of the spectra. Signals corresponding to different compounds and/or aggregates are highlighted in different colors.

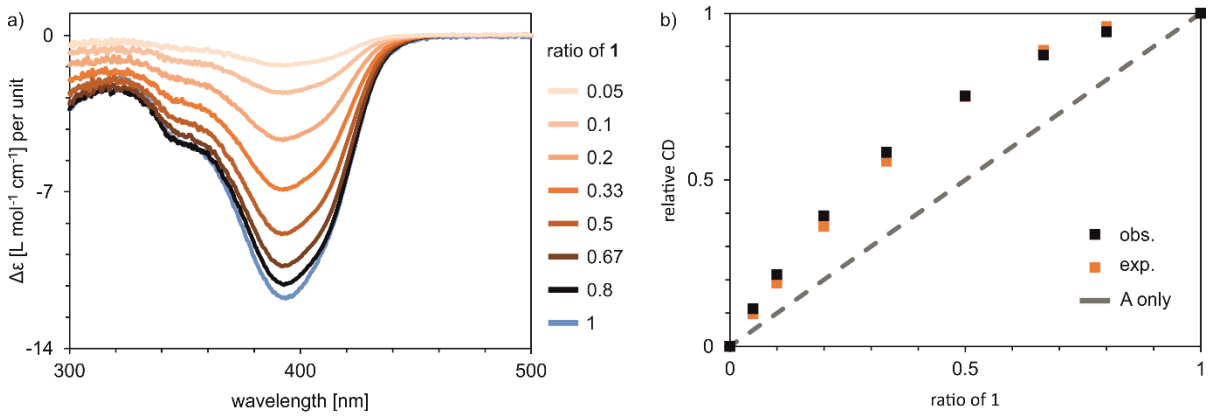

c)

ratio		complexes			CD	relative CD		
1	3	1-1	1-3	3-3	obs.	exp.	obs.	only A
1	0	1	0	0	-11.8	1.00	1.00	1.00
0.80	0.20	0.64	0.32	0.04	-11.1	0.96	0.94	0.80
0.67	0.33	0.44	0.44	0.11	-10.3	0.89	0.87	0.67
0.50	0.50	0.25	0.50	0.25	-8.85	0.75	0.75	0.50
0.33	0.67	0.11	0.44	0.44	-6.85	0.56	0.58	0.33
0.20	0.80	0.04	0.32	0.64	-4.62	0.36	0.39	0.20
0.10	0.90	0.01	0.18	0.81	-2.54	0.19	0.22	0.10
0.05	0.95	0.00	0.10	0.90	-1.32	0.10	0.11	0.05
0	1	0	0	1	0.00	0.00	0.00	0.00

Figure S14. a) CD spectra of mixtures of compounds **1** and **3** at total concentrations of 0.5 mM in H_2O. b) Observed (obs.) relative CD at the maxima of these mixtures plotted with the expected (exp.) values for stochastic heterodimer formation (orange) and no interaction (grey line). c) Table showing the ratios of stochastic dimer formation and the expected relative CD at different mixing ratios of compounds **1** and **3**.

2 Materials and Methods

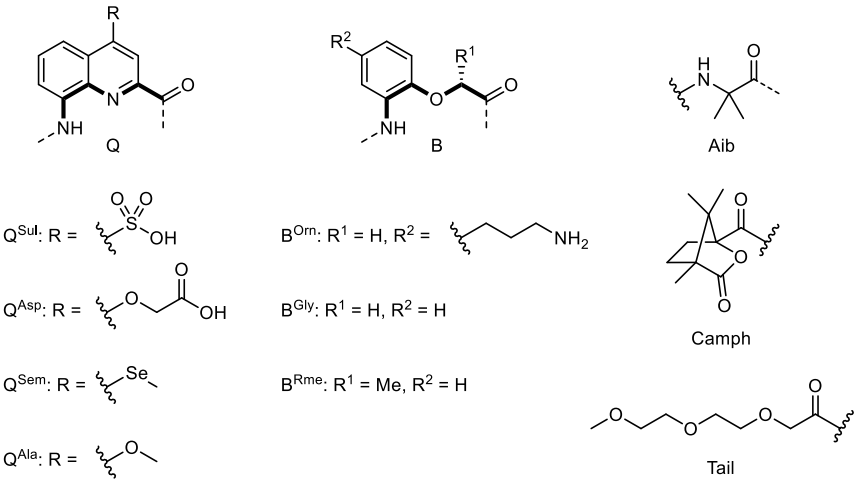

Figure S15. Fmoc-acid and other building blocks used in this study. Fmoc-Q^{Sul}-OH,[1] Fmoc-Q^{Asp}-OH,[2] Fmoc-Q^{Ala}-OH,[3] Fmoc-B^{Gly}-OH[4] and Fmoc-B^{Rme}-OH[4] have been described previously. Fmoc-Q^{Sem}-OH will be described elsewhere. For a detailed procedure to Fmoc-B^{Orn}(Boc)-OH (**13**), see section 2.3.

2.1 General

Commercial reagents (Suppliers: Abcr, Fisher Scientific, Merck, Sigma-Aldrich, TCI or VWR) were used without further purification unless otherwise stated. Cl-MPA ProTide™ resin LL and Rink Amide MBHA resin were purchased from CEM. Peptide grade *N*,*N*-dimethylformamide (DMF) was purchased from Carlo Erba. Anhydrous chloroform, triethylamine (TEA) and *N*,*N*-diisopropylethylamine (DIPEA) were obtained via distillation over CaH_2 prior to use. Anhydrous tetrahydrofuran (THF) and dichloromethane (DCM) were obtained via an MBRAUN SPS-800 solvent purification system. Ultrapure water was obtained via a Sartorius arium® pro VF ultrapure water system. Reactions were monitored by thin layer chromatography (TLC) on Merck silica gel 60-F254 plates and observed under UV light. Column chromatography purifications were carried out on Merck GEDURAN Si60 (40–63 μm). Nuclear magnetic resonance (NMR) spectra were recorded on an Avance III HD 400 MHz Bruker BioSpin spectrometer or an Avance III HD 500 MHz Bruker BioSpin spectrometer equipped with a broad band observe 5-mm BB-H&FD CryProbe™ Prodigy. Measurements were performed at 25 °C unless stated otherwise. In case of aqueous buffers and pure water solutions, mixtures of H_2O/D_2O 9/1 (*v/v*) were used, and water suppression was performed with excitation sculpting unless stated otherwise. Processing was done with MestReNova (v.12.0.0-20080) NMR processing software from Mestrelab Research. Chemical shifts are reported in ppm and calibrated via residual solvent signals or 3-(trimethylsilyl)propionic-2,2,3,3-d_4 acid sodium salt (TMSP) when water suppression was applied.[5] Signal multiplicities are abbreviated as s, singlet; d, doublet; t, triplet; q, quartet, and m, multiplet.

Signals were assigned using ^{1}H-^{13}C HMQC, ^{1}H-^{13}C HSQC and ^{1}H-^{13}C HMBC spectra using standard pulse sequences from the Bruker pulse program library applying standard processing parameters. Electrospray ionization (ESI) mass spectra were recorded on Bruker microTOF II and Thermo Finnigan LTQ FT Ultra spectrometers. Electron ionization (EI) mass spectra were recorded on a Thermo Q Exactive GC Orbitrap or a Finnigan MAT 95 sector mass spectrometer. Analytical and semi-preparative reversed phase (RP) high performance liquid chromatography (HPLC) was performed on a Thermo Fisher Scientific Ultimate 3000 HPLC System using Macherey-Nagel Nucleodur C18 Gravity columns (4 × 100 mm, 5 µm and 10 × 250 mm, 5 µm) and Macherey-Nagel Nucleodur C8 Gravity columns (4 × 50 mm, 5 µm and 10 × 100 mm, 5 µm). UV absorbance was monitored at 300 nm if not stated otherwise. Simple ultraviolet–visible (UV/Vis) absorbance measurements were done with a Thermo Fisher Scientific Nanodrop One instrument using a 1 cm quartz cuvette. Circular dichroism (CD) spectra were measured on a Jasco J-810 spectrometer. Measurements were performed at 20 °C if not stated otherwise. Manual microwave-assisted solid-phase foldamer synthesis (SPFS) was performed via a CEM® Discover Bio microwave peptide synthesizer. The temperature within the reactor vessel was monitored with an optical fiber probe. Automated SPFS was done via a Gyros Protein Technologies PurePep Chorus synthesizer with induction heating.

2.2 Solid phase synthesis procedures

Oligomers were synthesized according to previously reported SPFS protocols,[2, 6] hereafter referred to as standard method. Fmoc acid building blocks were activated *in situ* by generating the respective acid chlorides prior to coupling.

General acylation method: In the microwave vessel: after the resin (1.0 equiv.) was washed with anhydrous THF (4×), DIPEA (10.0 equiv.) and acyl chloride (5.0 equiv.) in anhydrous THF (1 mL per 100 mg resin; not less than 2 mL) were added and the suspension was heated to 50 °C for 15 min (25 W, ramp to 50 °C over 5 min, hold at 50 °C for 15 min). The resin was washed with anhydrous THF (3×) and the coupling step was repeated once. Then, the resin was washed again with anhydrous THF (1×) and DMF (5×), and kept suspended in DMF (if stored longer than 24 h, it was kept at 4 °C).

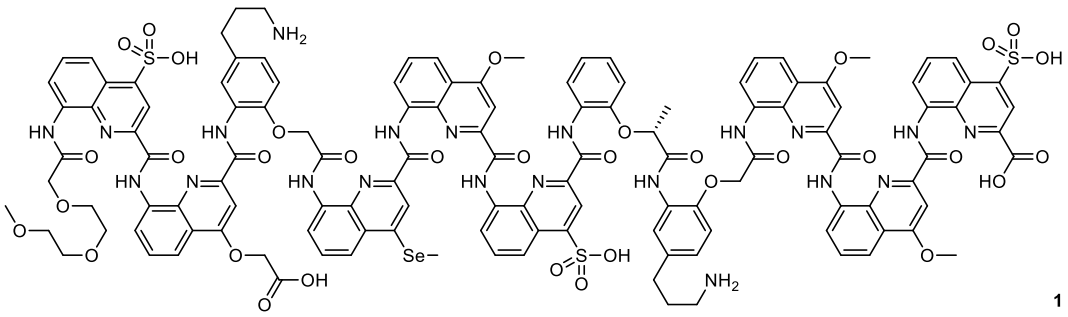

1

Compound 1: Oligomer **1** was synthesized on ProTide™ resin (0.16 mmol g^{-1}, 45 µmol scale) according to the standard method (manually). Loading of the first monomer: 0.11 mmol g^{-1} (71%). The final Tail group was installed via the standard method (using Tail-OH). After purification by semi-prep HPLC (C18, 0–25B, 50 °C; A: 13 mmol ammonium acetate buffer pH 8.5, B: acetonitrile), the title compound was obtained as a yellow solid (33.0 mg, 12.6 µmol, 28%; HPLC-purity: 98%). **^{1}H NMR** (500 MHz, 1 mM in 27 mM sodium phosphate aqueous buffer pH 7.0): δ = 11.04 (s, 3H), 10.88 (s, 1H), 10.69 (s, 1H), 9.90 (s, 1H), 9.70 (s, 1H), 9.30 (s, 1H), 8.69 (s, 1H), 8.60 (s, 1H), 8.27 (d, *J* = 9.5 Hz, 2H), 8.14 (d, *J* = 8.6 Hz, 1H), 8.04 (s, 1H), 7.96 (d, *J* = 9.3 Hz, 1H), 7.94–7.82 (m, 2H), 7.80–7.72 (m, 1H), 7.72–7.63 (m, 2H), 7.61 (d, *J* = 8.8 Hz, 1H), 7.49 (d, *J* = 9.2 Hz, 1H), 7.47–7.39 (m, 1H), 7.39–7.30 (m, 2H), 7.30–7.22 (m, 1H), 7.13 (s, 2H), 7.05 (s, 1H), 7.00 (s, 1H), 6.92–6.76 (m, 5H), 6.72 (s, 1H), 6.45 (d, *J* = 8.3 Hz, 1H), 6.28 (d, *J* = 9.6 Hz, 1H), 6.21 (s, 1H), 6.17 (s, 1H), 5.99 (s, 1H), 5.94 (s, 1H), 5.79–5.67 (m, 1H), 5.61 (s, 1H), 5.53 (s, 1H), 4.18 (s, 2H), 4.05 (s, 2H), 3.38 (d, *J* = 12.6 Hz, 1H), 3.29 (s, 4H), 2.98 (t, *J* = 8.6 Hz, 2H), 2.94–2.80 (m, 1H), 2.68 (s, 1H), 2.54 (s, 5H), 2.50–2.43 (m, 1H), 2.43–2.33 (m, 2H), 2.18 (s, 4H), 1.90–1.82 (m, 1H), 1.82–1.72 (m, 1H), 1.65–1.49 (m, 2H), 1.37–1.24 (m, 1H), -0.71 (d, *J* = 7.4 Hz, 3H). **HRMS** (ESI^-) *m/z* calcd. for $C_{124}H_{108}N_{21}O_{34}S_3Se$: 2610.5700 $(M-H)^-$; found: 2610.5909.

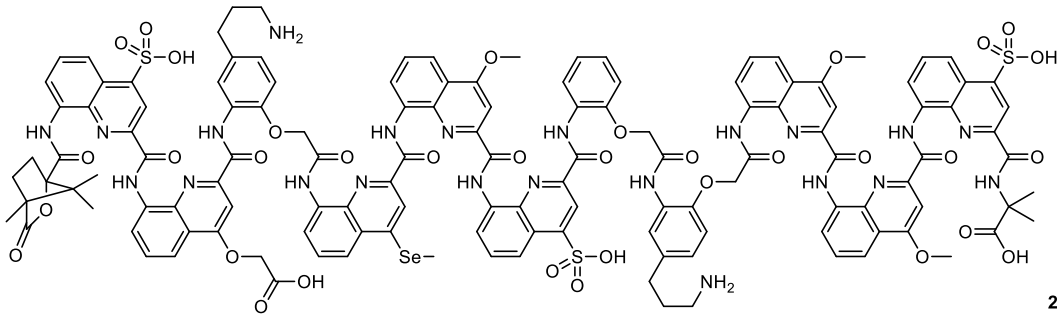

2

Compound 2: Oligomer **2** was synthesized on ProTide™ resin (0.16 mmol g^{-1}, 20 µmol scale) according to the standard method (manually). Loading of the first monomer: 0.16 mmol g^{-1} (quant.). The final **Camph** group was installed via the general acylation method. After purification by semi-prep HPLC (C18, 0–30B, 50 °C; A: 13 mmol ammonium acetate aqueous buffer pH 8.5, B: acetonitrile), the title compound was obtained as a yellow solid (18.0 mg, 6.67 µmol, 33%; HPLC-purity: 90%). **^{1}H NMR** (500 MHz, 1 mM in H_2O/D_2O 9:1): δ = 11.84 (s, 1H), 11.60 (s, 1H), 11.13 (s, 1H), 11.06 (s, 1H), 10.87 (s, 1H), 9.81 (s, 1H), 9.70 (s, 1H), 9.22 (s, 1H), 9.19 (s, 1H), 8.57 (s, 1H), 8.42 (d, *J* = 8.3 Hz, 1H), 8.33 (d, *J* = 8.3 Hz, 1H), 8.27 (d, *J* = 9.5 Hz, 2H), 8.23 (d, *J* = 8.5 Hz, 1H), 8.13 (s, 1H), 8.09 (d, *J* = 8.1 Hz, 1H), 8.04 (d, *J* = 9.0 Hz, 1H), 8.03–7.99 (m, 2H), 7.97–7.90 (m, 2H), 7.81 (d, *J* = 8.4 Hz, 1H), 7.77 (d, *J* = 9.3 Hz, 1H), 7.71–7.64 (m, 1H), 7.62 (d, *J* = 8.4 Hz, 1H), 7.60–7.46 (m, 5H), 7.44–7.37 (m, 2H), 7.35 (d, *J* = 8.5 Hz, 1H), 7.33–7.26 (m, 3H), 7.13 (d, *J* = 8.5 Hz, 1H), 7.11–7.05 (m, 1H), 7.04–7.00 (m, 2H), 6.99–6.94 (m, 2H), 6.93 (s, 1H), 6.82–6.68 (m, 8H), 6.66 (s, 2H), 6.34 (s, 1H), 6.32 (s, 2H), 6.30 (s, 1H), 6.23 (d, *J* = 9.3 Hz, 1H), 6.19 (d, *J* = 9.1 Hz, 1H), 4.00 (s, 3H), 3.96 (s, 3H), 3.94 (s, 3H), 3.54 (d, *J* = 15.6 Hz, 1H), 3.47 (d, *J* = 15.2 Hz, 1H), 3.23 (d, *J* = 16.0 Hz, 2H), 3.18 (t, *J* = 8.3 Hz, 3H), 3.00

(t, *J* = 8.4 Hz, 3H), 2.65–2.44 (m, 5H), 2.37 (s, 3H), 2.03–1.72 (m, 5H), 1.54 (dd, *J* = 19.0, 15.1 Hz, 3H), 1.37 (d, *J* = 15.0 Hz, 1H), 1.01 (s, 5H), 0.91 (s, 3H), 0.46 (s, 3H), 0.44 (s, 3H), -0.09 (s, 3H). **HRMS** (ESI^-) *m/z* calcd. for $C_{130}H_{113}N_{22}O_{34}S_3Se$: 2701.6122 $(M-H)^-$; found: 2701.7377.

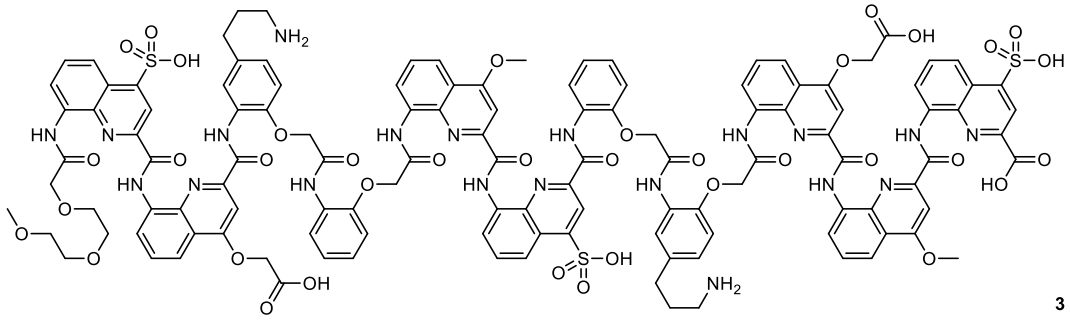

3

Compound 3: Oligomer **3** was synthesized on ProTide™ resin (0.23 mmol g^{-1}, 23 µmol scale) according to the standard method (manually). Loading of the first monomer: 0.23 mmol g^{-1} (98%). The final Tail group was installed via the standard method (using Tail-OH). After purification by semi-prep HPLC (C18, 0–20B, 25 °C; A: 13 mM ammonium acetate aqueous buffer pH 8.5, B: acetonitrile), the title compound was obtained as a yellow solid (10.4 mg, 4.11 µmol, 18%; HPLC-purity: >99%). **^{1}H NMR** (500 MHz, 0.5 mM in H_2O/D_2O 9:1): δ = 11.32 (s, 1H), 10.93 (s, 1H), 10.83 (s, 1H), 9.90 (s, 1H), 9.41 (s, 1H), 9.22 (s, 1H), 8.90 (s, 1H), 8.80 (s, 1H), 8.22 (d, *J* = 8.8 Hz, 1H), 8.16 (d, *J* = 7.9 Hz, 1H), 8.09 (d, *J* = 8.0 Hz, 1H), 8.07–8.01 (m, 2H), 7.97 (s, 1H), 7.83 (s, 1H), 7.81 (s, 2H), 7.73 (d, *J* = 9.1 Hz, 1H), 7.70 (s, 1H), 7.69 (s, 1H), 7.66–7.51 (m, 4H), 7.47 (t, *J* = 8.3 Hz, 1H), 7.36 (s, 1H), 7.31 (s, 1H), 7.25–7.15 (m, 3H), 7.14–6.97 (m, 5H), 6.92 (s, 1H), 6.84 (t, *J* = 7.8 Hz, 1H), 6.77 (t, *J* = 7.9 Hz, 1H), 6.70 (d, *J* = 8.3 Hz, 1H), 6.67 (d, *J* = 3.5 Hz, 1H), 6.61 (d, *J* = 7.7 Hz, 1H), 6.57–6.50 (m, 1H), 6.48 (d, *J* = 7.7 Hz, 1H), 6.42 (s, 1H), 6.35 (s, 1H), 6.19 (s, 1H), 6.08 (s, 1H), 6.04 (d, *J* = 8.9 Hz, 1H), 6.00 (d, *J* = 8.8 Hz, 1H), 5.95 (d, *J* = 8.6 Hz, 1H), 5.77 (d, *J* = 6.8 Hz, 1H), 3.79 (s, 3H), 3.45 (s, 3H), 3.36 (d, *J* = 13.9 Hz, 1H), 3.23 (d, *J* = 14.4 Hz, 1H), 3.10–2.83 (m, 8H), 2.67–2.60 (m, 2H), 2.58 (s, 3H), 2.57–2.42 (m, 6H), 2.32–2.19 (m, 3H), 2.06 (s, 2H), 1.80 (qt, *J* = 14.4, 7.5 Hz, 1H), 1.64 (t, *J* = 10.3 Hz, 1H), 1.43 (d, *J* = 14.6 Hz, 1H), 1.36–1.21 (m, 1H), 0.97–0.85 (m, 2H). **HRMS** (ESI^-) *m/z* calcd. for $C_{121}H_{105}N_{20}O_{37}S_3$: 2525.6117 $(M-H)^-$; found: 2525.5560.

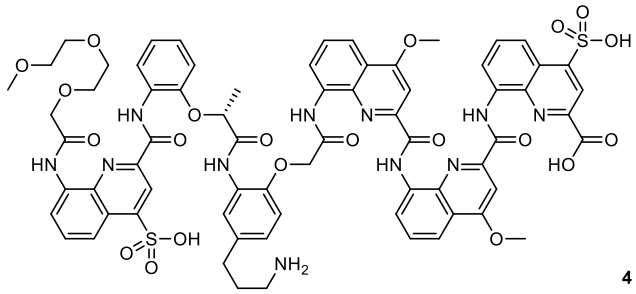

4

Compound 4: Oligomer **4** was synthesized on ProTide™ resin (0.15 mmol g^{-1}, 25 µmol scale) according to the standard method (automated). Loading of the first monomer: 0.13 mmol g^{-1} (88%). The final Tail group was installed via the standard method (using Tail-OH). After purification by semi-prep

HPLC (C18, 0–30B, 50 °C; A: 13 mM ammonium acetate aqueous buffer pH 8.5, B: acetonitrile), the title compound was obtained as a yellow solid (1.24 mg, 0.859 µmol, 14%; HPLC-purity: >99%). **^{1}H NMR** (500 MHz, 1 mM in 27 mmol sodium phosphate aqueous buffer pH 7.0): δ = 11.39 (s, 2H), 9.79 (s, 1H), 9.43 (s, 1H), 9.35 (s, 1H), 8.22 (d, *J* = 10.3 Hz, 1H), 8.17 (s, 1H), 8.12–8.00 (m, 1H), 7.93 (d, *J* = 9.1 Hz, 1H), 7.82 (d, *J* = 6.0 Hz, 4H), 7.68–7.52 (m, 3H), 7.36–7.21 (m, 2H), 7.21–7.03 (m, 3H), 6.98–6.88 (m, 1H), 6.86 (s, 1H), 6.84–6.73 (m, 1H), 6.57 (d, *J* = 7.3 Hz, 1H), 6.49 (t, *J* = 8.3 Hz, 2H), 6.44 (d, *J* = 8.6 Hz, 1H), 6.36 (s, 1H), 5.79 (d, *J* = 10.3 Hz, 1H), 4.22 (s, 2H), 3.57 (s, 4H), 3.54–3.45 (m, 1H), 3.45–3.31 (m, 1H), 3.27–3.12 (m, 3H), 3.07 (s, 3H), 2.89 (d, *J* = 13.7 Hz, 3H), 2.74 (s, 4H), 2.68 (s, 5H), 2.63–2.51 (m, 4H), 2.40–2.14 (m, 4H), 1.99 (s, 4H), 1.79–1.56 (m, 3H), 1.42 (d, *J* = 17.2 Hz, 1H), 1.36–1.20 (m, 5H). **HRMS** (ESI$^-$) *m/z* calcd. for $C_{69}H_{64}N_{11}O_{21}S_2$: 1446.3725 $(M\text{-}H)^-$; found: 1446.4677.

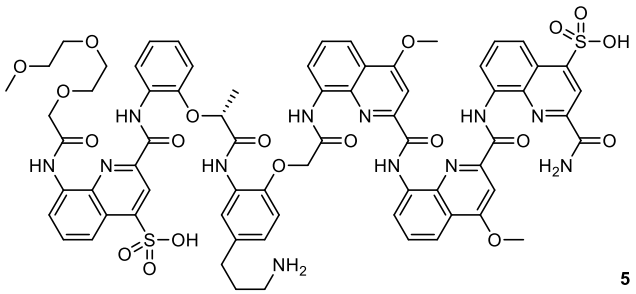

5

Compound 5: Oligomer **5** was synthesized on Rink Amide MBHA resin (0.33 mmol g^{-1}, 25 µmol scale) according to the standard method (automated). Loading of the first monomer: 0.33 mmol g^{-1} (quant.). The final Tail group was installed via the standard method (using Tail-OH). After purification by semi-prep HPLC (C18, 0–40B, 50 °C; A: 13 mmol ammonium acetate aqueous buffer pH 8.5, B: acetonitrile), the title compound was obtained as a yellow solid (18.5 mg, 12.8 µmol, 51%; HPLC-purity: 96%). **^{1}H NMR** (500 MHz, 1 mM in 12 mM ammonium acetate aqueous buffer pH 8.5): δ = 11.40 (s, 1H), 10.71 (s, 1H), 9.79 (s, 1H), 9.44 (s, 1H), 9.28 (s, 1H), 8.40 (d, *J* = 8.6 Hz, 1H), 8.22 (d, *J* = 9.2 Hz, 1H), 8.18 (d, *J* = 9.5 Hz, 1H), 8.14 (d, *J* = 15.4 Hz, 3H), 8.04 (d, *J* = 8.4 Hz, 1H), 7.66 (d, *J* = 8.9 Hz, 1H), 7.64–7.60 (m, 2H), 7.58 (d, *J* = 8.6 Hz, 1H), 7.25 (d, *J* = 9.1 Hz, 1H), 7.19 (t, *J* = 8.5 Hz, 1H), 7.15–7.06 (m, 4H), 6.95 (d, *J* = 8.2 Hz, 1H), 6.93–6.84 (m, 3H), 6.76 (s, 1H), 6.69 (d, *J* = 9.0 Hz, 1H), 6.55 (t, *J* = 8.5 Hz, 1H), 6.46 (d, *J* = 9.6 Hz, 1H), 6.16 (s, 1H), 5.88 (d, *J* = 9.3 Hz, 1H), 3.51 (d, *J* = 15.5 Hz, 1H), 3.47–3.34 (m, 6H), 3.28–3.16 (m, 3H), 3.15–3.05 (m, 3H), 2.87 (t, *J* = 8.6 Hz, 2H), 2.79 (dt, *J* = 13.0, 4.8 Hz, 1H), 2.71 (s, 3H), 2.66–2.54 (m, 3H), 2.32–2.13 (m, 3H), 1.74–1.53 (m, 2H), 1.40 (d, *J* = 15.9 Hz, 1H), 1.33 (d, *J* = 6.7 Hz, 4H), 1.27 (t, *J* = 7.9 Hz, 1H). **HRMS** (ESI$^-$) *m/z* calcd. for $C_{69}H_{65}N_{12}O_{20}S_2$: 1445.3885 $(M\text{-}H)^-$; found: 1445.3797.

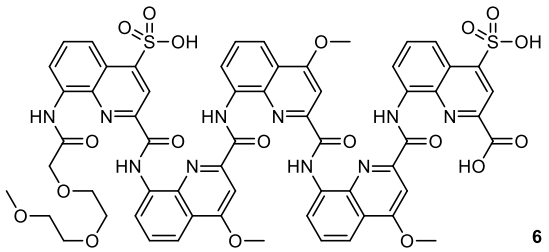

6

Compound 6: Oligomer **6** was synthesized on ProTide™ resin (0.15 mmol g^{-1}, 25 µmol scale) according to the standard method (manually). Loading of the first monomer: 0.13 mmol g^{-1} (88%). The final Tail group was installed via the standard method (using Tail-OH). After purification by semi-prep HPLC (C18, 0–50B, 50 °C; A: 13 mmol ammonium acetate aqueous buffer pH 8.5, B: acetonitrile), the title compound was obtained as a yellow solid (11.3 mg, 8.82 µmol, 35%; HPLC-purity: 98%). **^{1}H NMR** (500 MHz, 1 mM in 12 mM ammonium acetate aqueous buffer pH 8.5): δ = 12.05 (s, 1H), 11.92 (s, 1H), 11.86 (s, 1H), 11.65 (s, 1H), 9.94 (s, 1H), 8.61 (d, *J* = 9.3 Hz, 1H), 8.53–8.30 (m, 4H), 8.14 (d, *J* = 10.2 Hz, 1H), 8.09 (d, *J* = 8.8 Hz, 1H), 8.01 (d, *J* = 9.0 Hz, 1H), 7.98–7.78 (m, 2H), 7.73 (d, *J* = 6.2 Hz, 1H), 7.67–7.57 (m, 2H), 7.52 (d, *J* = 8.5 Hz, 2H), 7.44 (t, *J* = 9.4 Hz, 1H), 6.93 (s, 1H), 6.84 (s, 1H), 4.15 (s, 2H), 4.12 (s, 2H), 3.59–3.34 (m, 3H), 3.10–2.97 (m, 1H), 2.94–2.83 (m, 1H), 2.74 (s, 4H), 2.67 (s, 3H), 2.57 (d, *J* = 14.7 Hz, 1H), 2.53–2.33 (m, 2H). **HRMS** (ESI^-) *m/z* calcd. for $C_{60}H_{49}N_{10}O_{19}S_2$: 1277.2622 $(M-H)^-$; found: 1277.3584.

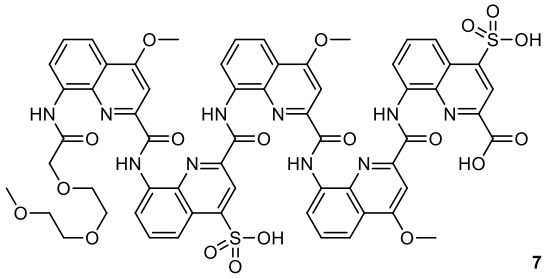

7

Compound 7: Oligomer **7** was synthesized on ProTide™ resin (0.15 mmol g^{-1}, 25 µmol scale) according to the standard method (automated). Loading of the first monomer: 0.11 mmol g^{-1} (74%). The final Tail group was installed via the standard method (using Tail-OH). After purification by semi-prep HPLC (C18, 0–50B, 50 °C; A: 13 mmol ammonium acetate aqueous buffer pH 8.5, B: acetonitrile), the title compound was obtained as a yellow solid (13.2 mg, 10.3 µmol, 41%; HPLC-purity: 96%). **^{1}H NMR** (500 MHz, 5 mM in 27 mM sodium phosphate aqueous buffer pH 7.0): δ = 11.04 (s, 1H), 10.95 (s, 1H), 10.93 (s, 1H), 10.90 (s, 1H), 9.23 (s, 1H), 8.18 (d, *J* = 10.0 Hz, 1H), 8.01 (s, 1H), 7.89 (d, *J* = 10.1 Hz, 1H), 7.71 (d, *J* = 8.8 Hz, 1H), 7.59–7.46 (m, 3H), 7.46–7.37 (m, 2H), 7.35 (d, *J* = 8.6 Hz, 1H), 7.23 (d, *J* = 7.4 Hz, 1H), 7.19 (d, *J* = 7.7 Hz, 1H), 7.16–7.03 (m, 2H), 6.95 (t, *J* = 8.5 Hz, 1H), 6.77 (s, 1H), 6.73 (s, 1H), 6.34 (s, 1H), 6.13 (s, 1H), 4.01 (s, 3H), 3.90 (s, 4H), 3.62 (s, 3H), 3.22–3.04 (m, 3H), 2.75–2.60 (m, 4H), 2.60–2.40 (m, 7H), 2.30–2.20 (m, 1H), 2.15–2.04 (m, 2H), 1.41 (t, *J* = 11.7 Hz, 1H). **HRMS** (ESI^-) *m/z* calcd. for $C_{60}H_{49}N_{10}O_{19}S_2$: 1277.2622 $(M-H)^-$; found: 1277.2303.

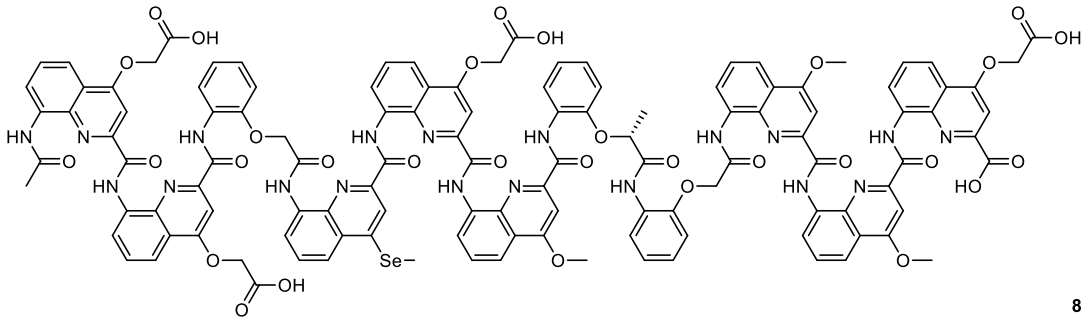

8

Compound 8: The synthesis of this oligomer has already been published previously.[4]

2.3 Monomer synthesis procedures

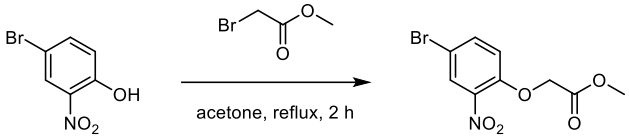

Compound 9: 4-Bromo-2-nitrophenol (10.0 g, 45.9 mmol, 1.0 equiv.), methyl bromoacetate (4.78 ml, 50.5 mmol, 1.1 equiv.) and K_2CO_3 (6.97 g, 50.5 mmol, 1.1 equiv.) were suspended in anhydrous acetone (180 ml). The reaction mixture was refluxed (bath temp.: 75 °C) for 2 h, filtered and solvents were evaporated *in vacuo*. Then, the residue was diluted with H_2O, extracted with DCM (2×) and the combined organic phases were dried over $MgSO_4$. After removing the solvents *in vacuo*, the title compound (13.7 g, 45.9 mmol, quant.) was obtained as a light-yellow solid. ($C_9H_8BrNO_5$, MW = 290.07 g mol^{-1}). $\mathbf{R_f}$ (CyHex/EtOAc 9:1) = 0.11. **^{1}H NMR** (500 MHz, $CDCl_3$): δ = 7.99 (d, *J* = 2.46 Hz, 1H, C3-H), 7.62 (dd, *J* = 8.94 Hz, 2.47 Hz, 1H, C5-H), 6.89 (d, *J* = 8.93 Hz, 1H, C6-H), 4.77 (s, 2H, C7-H), 3.80 (s, 3H, C9-H). **^{13}C NMR** (500 MHz, $CDCl_3$): δ = 168.0 (C8), 150.5 (C1), 140.9 (C2), 136.9 (C5), 128.7 (C3), 117.0 (C6), 113.7 (C4), 66.7 (C7), 52.7 (C9). **HRMS** (ESI$^+$) *m/z* calcd. for $C_9H_9BrNO_5$: 289.9659 $(M+H)^+$; Found: 289.9666.

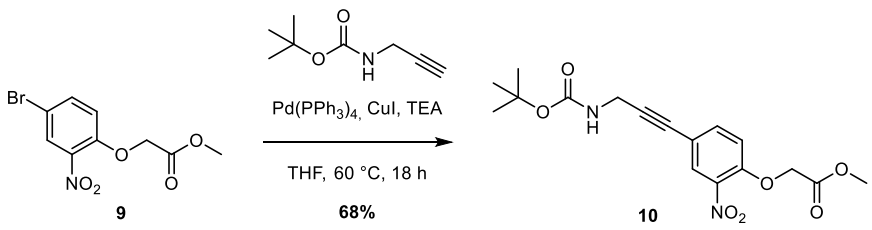

Compound 10: Compound **9** (5.73 g, 19.8 mmol, 1.0 equiv.), *N*-Boc-propargylamine (4.60 g, 29.6 mmol, 1.5 equiv.) and TEA (6.89 ml, 49.4 mmol, 2.5 equiv.) were dissolved in anhydrous THF (80 ml). The solution was degassed by freeze pump cycles (3×) and put under Ar atmosphere. Then, CuI (188 mg, 988 µmol, 5 mol%) and $Pd(PPh_3)_4$ (1.14 g, 988 µmol, 5 mol%) were added and the reaction mixture was stirred at 60 °C for 18 h. After diluting with H_2O, the mixture was extracted with DCM

(3×), dried over $MgSO_4$ and solvents were removed *in vacuo*. The residue was triturated in Et_2O/CyHex 9:1, filtered and washed with CyHex. Finally, the precipitate was purified further by column chromatography (SiO_2, CyHex/EtOAc 8:2 → 6:4) yielding the title compound as a white solid (4.86 g, 13.3 mmol, 68%). ($C_{17}H_{20}N_2O_7$, MW = 364.35 g mol^{-1}). **R_f** (CyHex/EtOAc 6:4) = 0.39. **^{1}H NMR** (500 MHz, $CDCl_3$): δ = 7.91 (d, *J* = 2.08 Hz, 1H, C3-H), 7.53 (dd, *J* = 8.70 Hz, 2.12 Hz, 1H, C5-H), 6.90 (d, *J* = 8.69 Hz, 1H, C6-H), 4.79 (s, 2H, C7-H), 4.76 (s, 1H, N13-H), 4.14 (d, *J* = 5.69 Hz, 2H, C12-H), 3.81 (s, 3H, C9-H), 1.47 (s, 9H, C16-H, C17-H, C18-H). **^{13}C NMR** (500 MHz, $CDCl_3$): δ = 168.0 (C8), 155.4 (C14), 151.0 (C1), 140.2 (C2), 137.1 (C5), 129.2 (C3), 117.0 (C4), 115.1 (C6), 87.1 (C11), 80.4 (C10, C15), 66.5 (C7), 52.8 (C9), 31.2 (C13), 28.5 (C16, C17, C18). **HRMS** (ESI^+) *m/z* calcd. for $C_{17}H_{20}N_2O_7Na$: 387.1163 $(M+Na)^+$; Found: 387.1163.

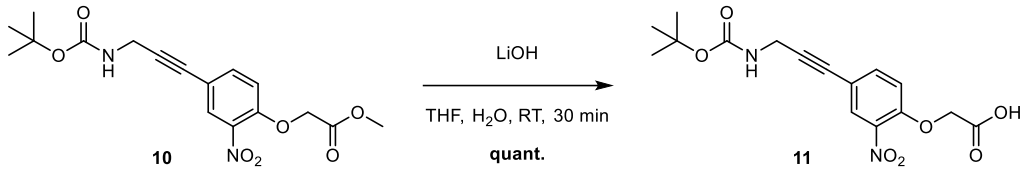

Compound 11: Compound **10** (2.45 g, 6.72 mmol, 1.0 equiv.) was dissolved in THF (100 ml). After the addition of LiOH (193 mg, 8.07 mmol, 1.2 equiv.) in H_2O (25 ml), the solution was stirred at RT for 30 min. Then, the mixture was acidified using citric acid $_{(aq.)}$ (1 M). The resulting solution was extracted with DCM (3×) and dried over $MgSO_4$. After removing the solvents *in vacuo*, the title compound was obtained as a white solid (2.36 g, 6.72 mmol, quant.). ($C_{16}H_{18}N_2O_7$, MW = 350.33 g mol^{-1}). **^{1}H NMR** (500 MHz, DMSO-d_6): δ = 13.32 (s, 1H, O9-H), 7.90 (d, *J* = 2.15 Hz, 1H, C3-H), 7.63 (dd, *J* = 8.82 Hz, 2.20 Hz, 1H, C5-H), 7.36 (t, *J* = 5.74 Hz, 1H, N13-H), 7.24 (d, *J* = 8.81 Hz, 1H, C6-H), 4.92 (s, 2H, C7-H), 3.97 (d, *J* = 5.71 Hz, 2H, C12-H), 1.40 (s, 9H, C16-H, C17-H, C18-H). **^{13}C NMR** (500 MHz, DMSO-d_6): δ = 169.1 (C8), 155.3 (C14), 150.3 (C1), 139.5 (C2), 136.6 (C5), 127.5 (C3), 115.7 (C6), 114.9 (C4), 88.1 (C11), 79.1 (C10), 78.3 (C15), 65.5 (C7), 30.1 (C12), 28.2 (C16, C17, C18). **HRMS** (ESI^-) *m/z* calcd. for $C_{16}H_{17}N_2O_7$: 349.1041 $(M-H)^-$; Found: 349.1040.

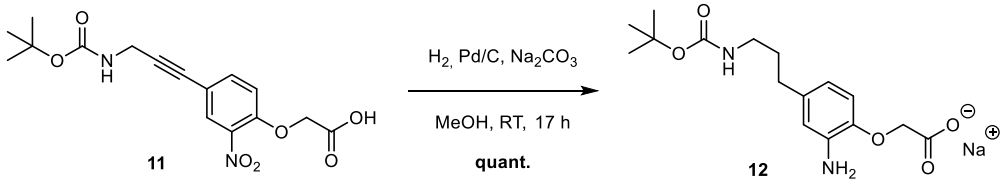

Compound 12: Compound **11** (2.36 g, 6.74 mmol, 1.0 equiv.) and Na_2CO_3 (713 mg, 6.74 mmol, 1.0 equiv.) were suspended in MeOH (250 ml). After the solution was quickly degassed by vacuum–N_2 cycles (3×), Pd/C (236 mg, 10 wt. % loading) was added and the N_2 atmosphere was replaced by H_2. The reaction mixture was stirred at RT for 17 h, filtered over Celite© and washed with MeOH. Solvents were evaporated *in vacuo* yielding the title compound as a light-yellow solid (2.33 g, 6.74 mmol, 1.0 equiv.). ($C_{16}H_{23}N_2O_5Na$, MW = 346.36 g mol^{-1}). **^{1}H NMR** (500 MHz, DMSO-d_6): δ = 6.80 (t, *J* = 5.73 Hz, 1H, N14-H), 6.53 (d, *J* = 8.04 Hz, 1H, C6-H), 6.40 (d, *J* = 2.09 Hz, 1H, C3-H), 6.23 (dd, *J* =

8.10 Hz, 2.13 Hz, 1H, C5-H), 4.90 (s, 2H, N10-H), 3.98 (s, 2H, C7-H), 2.89 (q, *J* = 6.67 Hz, 2H, C13-H), 2.33 (t, *J* = 7.72 Hz, 2H, C11-H), 1.57 (p, *J* = 7.38 Hz, 2H, C12-H), 1.37 (s, 9H, C17-H, C18-H, C19-H). **^{13}C NMR** (500 MHz, DMSO-d_6): δ = 171.4 (C8), 155.6 (C15), 145.4 (C1), 139.0 (C2), 134.1 (C4), 115.7 (C5), 114.5 (C6), 114.1 (C3), 77.3 (C16), 70.8 (C7), 39.5 (C13), 32.2 (C11), 31.6 (C12), 28.3 (C17, C18, C19). **HRMS** (ESI^-) *m/z* calcd. for $C_{16}H_{22}N_2O_5$: 323.1612 $(M-H)^-$; Found: 323.1610.

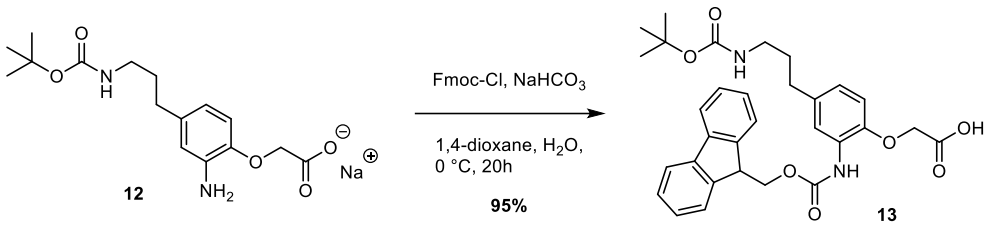

Compound 13: Compound **12** (2.33 g, 6.74 mmol, 1.0 equiv.) and $NaHCO_3$ (2.83 g, 33.7 mmol, 5.0 equiv.) were dissolved in H_2O (150 ml). Then, Fmoc-Cl (2.27 g, 8.76 mmol, 1.3 equiv.) in 1,4-dioxane (150 ml) were added at 0 °C over 1 h. The reaction mixture was stirred at 0 °C for 1 h and then at RT for 18 h. After the mixture was acidified using citric acid $_{(aq.)}$ (1 M), it was extracted with DCM (3×), dried over $MgSO_4$ and solvents were removed *in vacuo*. The residue was purified by column chromatography (SiO_2, CyHex/EtOAc 1:1 + 1% DIPEA → CyHex/EtOAc 1:1 → CyHex/EtOAc 1:1 + 1% AcOH → EtOAc + 1% AcOH) to yield the title compound as a white solid (3.51 g, 6.42 mmol, 95%). ($C_{31}H_{34}N_2O_7$, MW = 546.62 g mol^{-1}). $\mathbf{R}_f$ (EtOAc/MeOH 98:2 + 1% AcOH) = 0.36. **^{1}H NMR** (500 MHz, DMSO-d_6): δ = 13.08 (s, 1H, O9-H), 8.65 (s, 1H, N19-H), 7.91 (dt, *J* = 7.57, 0.97 Hz, 2H, C25-H, C27-H), 7.74 (d, *J* = 7.44 Hz, 2H, C23-H, C30-H), 7.52 (s, 1H, C3-H), 7.43 (td, *J* = 7.46, 1.14 Hz, 2H, C25-H, C28-H), 7.34 (td, *J* = 7.49, 1.18 Hz, 2H, C24-H, C29-H), 6.89 (d, *J* = 8.39 Hz, 1H, C6-H), 6.87–6.82 (m, 2H, C5-H, N13-H), 4.69 (s, 2H, C7-H), 4.41 (d, *J* = 7.11 Hz, 2H, C21-H), 4.31 (t, *J* = 7.06 Hz, 1H, C22-H), 2.92 (q, *J* = 6.65 Hz, 2H, C12-H), 2.48–2.41 (m, 2H, C10-H), 1.61 (quint., *J* = 7.30 Hz, 2H, C11-H), 1.37 (s, 9H, C16-H, C17-H, C18-H). **^{13}C NMR** (500 MHz, DMSO-d_6): δ = 170.7 (C8), 155.6 (C14), 153.5 (C20), 146.7 (C1), 143.8 (C22a, C30a), 140.7 (C26a, C26b), 135.0 (C4), 127.7 (C25, C28), 127.5 (C2), 127.1 (C24, C29), 125.3 (C23, C30), 123.7 (C5), 120.2 (C26, C27), 113.6 (C6), 77.4 (C15), 66.4 (C7), 66.1 (C21), 46.6 (C22), 39.4 (C12), 32.0 (C10), 31.5 (C11), 28.3 (C16, C17, C18). **HRMS** (ESI^-) *m/z* calcd. for $C_{31}H_{33}N_2O_7$: 545.2293 $(M-H)^-$; Found: 545.2289.

3 Advanced NMR measurements

3.1 Assignment of oligomer 1

The 2D NOESY spectrum was recorded on a Avance III HD 500 MHz Bruker BioSpin spectrometer equipped with a broad band observe 5-mm BB-H&FD CryProbe™ Prodigy with a phase-sensitive pulse sequence with water suppression employing an excitation sculpting element from the Bruker pulse program library (noesyesfpgpphrs). Data acquisition was performed with 1K (F2) x 512 (F1) data points and a mixing time of 0.5 s. The recycling delay was 1.5 s and 16 transients per increment were applied at a sweep width of 8 kHz in both dimensions resulting in an acquisition time of 0.1204 s. The special acquisition parameters regarding the water suppression element of the pulse sequence were adopted from the optimized parameter set of the respective one-dimensional experiment. A 90° shifted sine-square multiplication, an exponential window of 1.0 Hz as well as a gaussian window of 1 Hz in both dimensions prior to FT was applied.

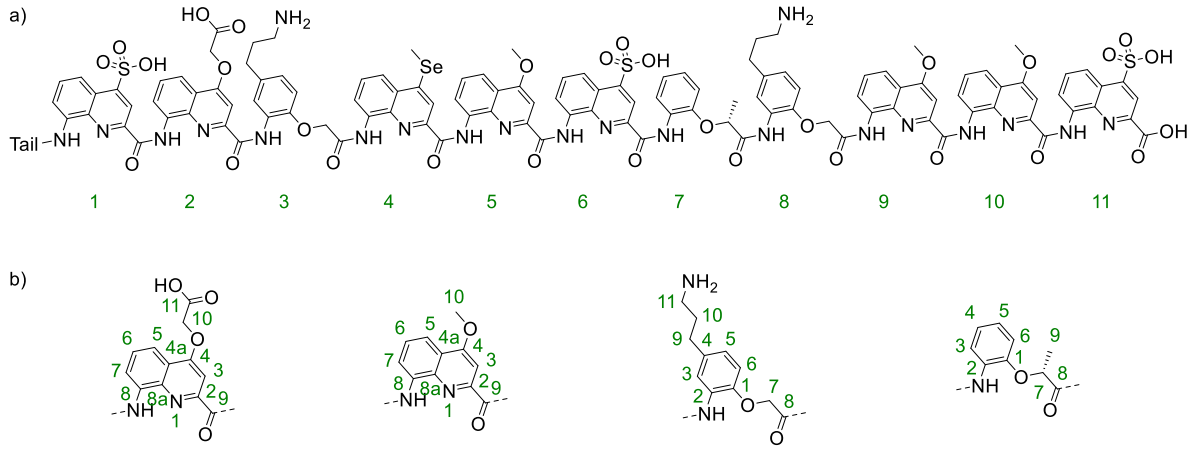

Figure S16. a) Numbering of the units of compound **1** used in NMR assignment. b) Representative numbering of the carbon atoms in Q- and B-units.

Table S1. Assignment of the ^{1}H chemical shifts of compound **1** in 27 mM sodium phosphate aqueous buffer pH 7.0 H_2O/D_2O 9:1 at 25 °C (500 MHz).

Monomer	Atom	^{1}H (ppm)	Monomer	Atom	^{1}H (ppm)
Q1 (Sul)	H3	8.05	B7 (Rme)	H3	6.46
	H5	8.29		H4	5.61
	H6	7.68		H5	5.67
	H7	8.16		H6	5.51
	NH	9.93		H7	2.82
				H9	-0.71
				NH	8.71
Q2 (Asp)	H3	7.04	B8 (Orn)	H3	5.92
	H5	7.86		H5	5.73
	H6	7.34		H6	5.12
	H7	7.62		H7	3.05; 2.02
	H10	4.87; 4.75		H9	1.75
	NH	11.60		H10	1.32
				H11	2.88
				NH	6.15
B3 (Orn)	H3	7.35	Q9 (Ala)	H3	7.14
	H5	6.82		H5	7.50
	H6	6.30		H6	7.00
	H7	3.34; 1.61		H7	6.86
	H9	3.34; 1.61		H10	4.19
	H10	1.84		NH	8.60
	H11	2.99			
	NH	9.72			
Q4 (Sem)	H3	6.21	Q10 (Ala)	H3	5.99
	H5	7.46		H5	6.84
	H6	7.27		H6	6.80
	H7	6.88		H7	7.27
	H10	2.18		H10	3.29
	NH	9.32		NH	10.88
Q5 (Ala)	H3	6.88	Q11 (Sul)	H3	6.72
	H5	7.89		H5	7.65
	H6	7.64		H6	7.14
	H7	7.91		H7	7.77
	H10	4.05		NH	11.07
	NH	11.6			
Q6 (Sul)	H3	7.00			
	H5	7.96			
	H6	7.42			
	H7	8.27			
	NH	10.7			

Table S2. Assignment of the ^{13}C chemical shifts of compound **1** in 27 mM sodium phosphate aqueous buffer pH 7.0 H_2O/D_2O 9:1 at 25 °C (500 MHz).

Monomer	Atom	^{13}C (ppm)	Monomer	Atom	^{13}C (ppm)
Q1 (Sul)	C3	120.0	B7 (Rme)	C1	149.3
	C4	152.4		C3	120.1
	C4a	127.3		C4	124.7
	C5	123.8		C5	127.0
	C6	133.3		C6	117.0
	C7	120.4		C7	81.8
	C8	136.4		C8	168.3
	C8a	139.8		C9	16.4
Q2 (Asp)	C3	102.4	B8 (Orn)	C1	142.4
	C4	166.2		C2	135.0
	C4a	124.4		C3	118.4
	C5	119.8		C4	126.0
	C6	130.8		C5	125.6
	C7	119.6		C6	111.4
	C8	133.7		C7	68.3
	C8a	139.9		C9	32.7
	C10	70.6		C10	29.1
				C11	42.5
B3 (Orn)	C1	145.0	Q9 (Ala)	C3	102.0
	C2	137.4		C4	167.0
	C3	119.8		C4a	123.5
	C4	127.7		C5	119.2
	C5	127.3		C6	130.4
	C6	113.5		C7	119.4
	C7	68.2		C8	132.7
	C9	34.0		C8a	138.5
	C10	31.4		C10	59.5
	C11	42.0			
Q4 (Sem)	C3	117.3	Q10 (Ala)	C3	100.3
	C4	153.7		C4	164.6
	C4a	130.5		C4a	122.8
	C5	123.1		C5	119.1
	C6	131.7		C6	130.7
	C7	119.6		C7	117.8
	C8	133.4		C8	134.3
	C8a	136.4		C8a	134.4
	C10	8.2		C10	58.6
Q5 (Ala)	C3	101.1	Q11 (Sul)	C3	120.3
	C4	166.9		C4	152.9
	C4a	125.1		C4a	125.3
	C5	119.8		C5	123.5
	C6	131.0		C6	131.8
	C7	119.8		C7	118.1
	C8	134.8		C8	135.9
	C8a	140.7		C8a	139.9
	C10	59.3			
Q6 (Sul)	C3	117.9			
	C4	152.4			
	C4a	126.7			
	C5	123.9			
	C6	132.9			
	C7	119.9			
	C8	135.0			
	C8a	139.2			

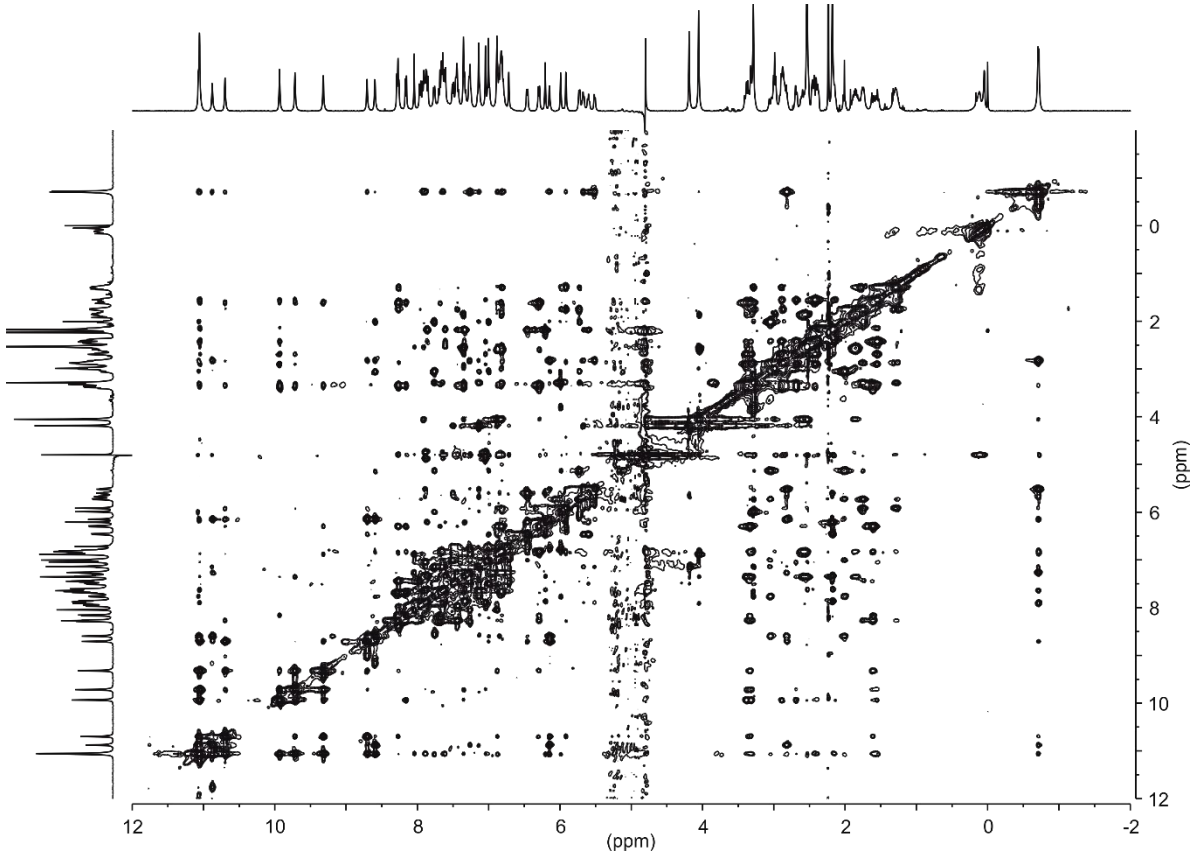

Figure S17. ^{1}H-^{1}H NOESY spectrum of **1** (500 MHz, 27 mM sodium phosphate aqueous buffer pH 7.0).

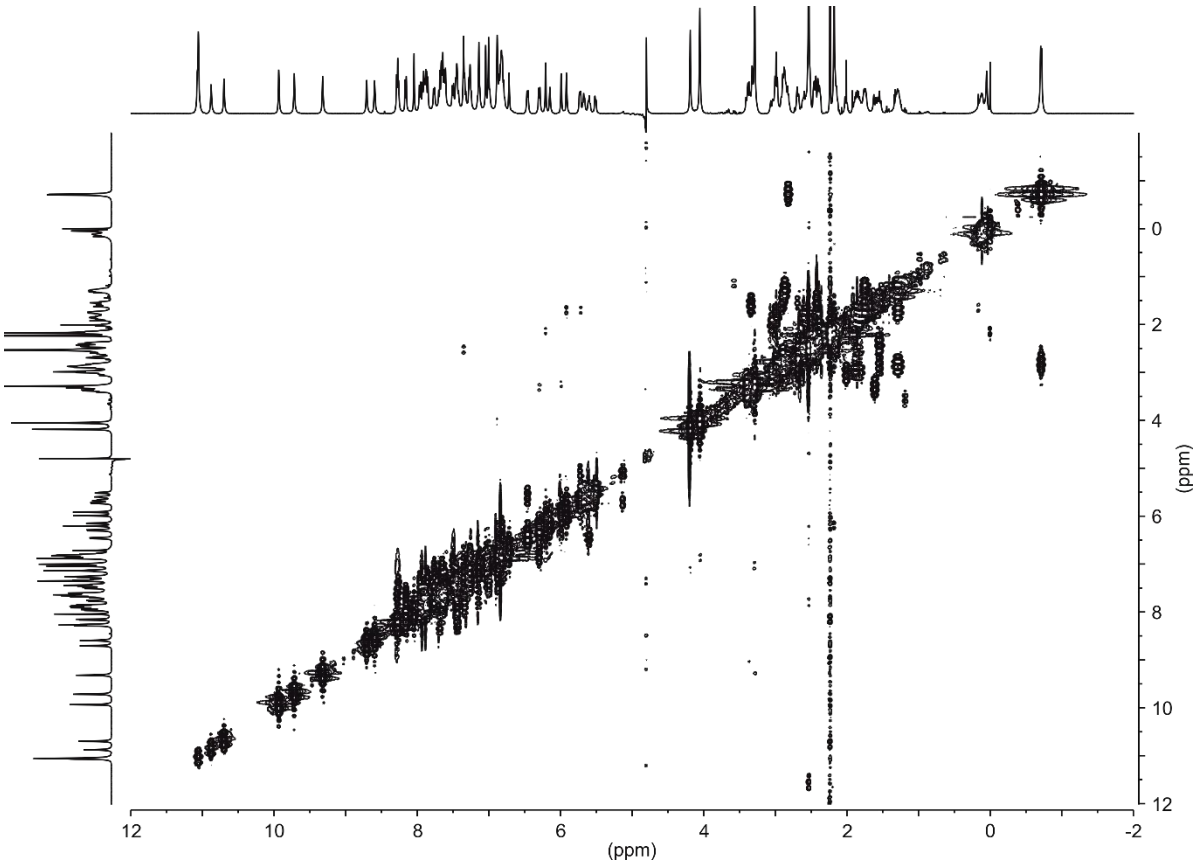

Figure S18. ^{1}H-^{1}H COSY spectrum of **1** (500 MHz, 27 mM sodium phosphate aqueous buffer pH 7.0).

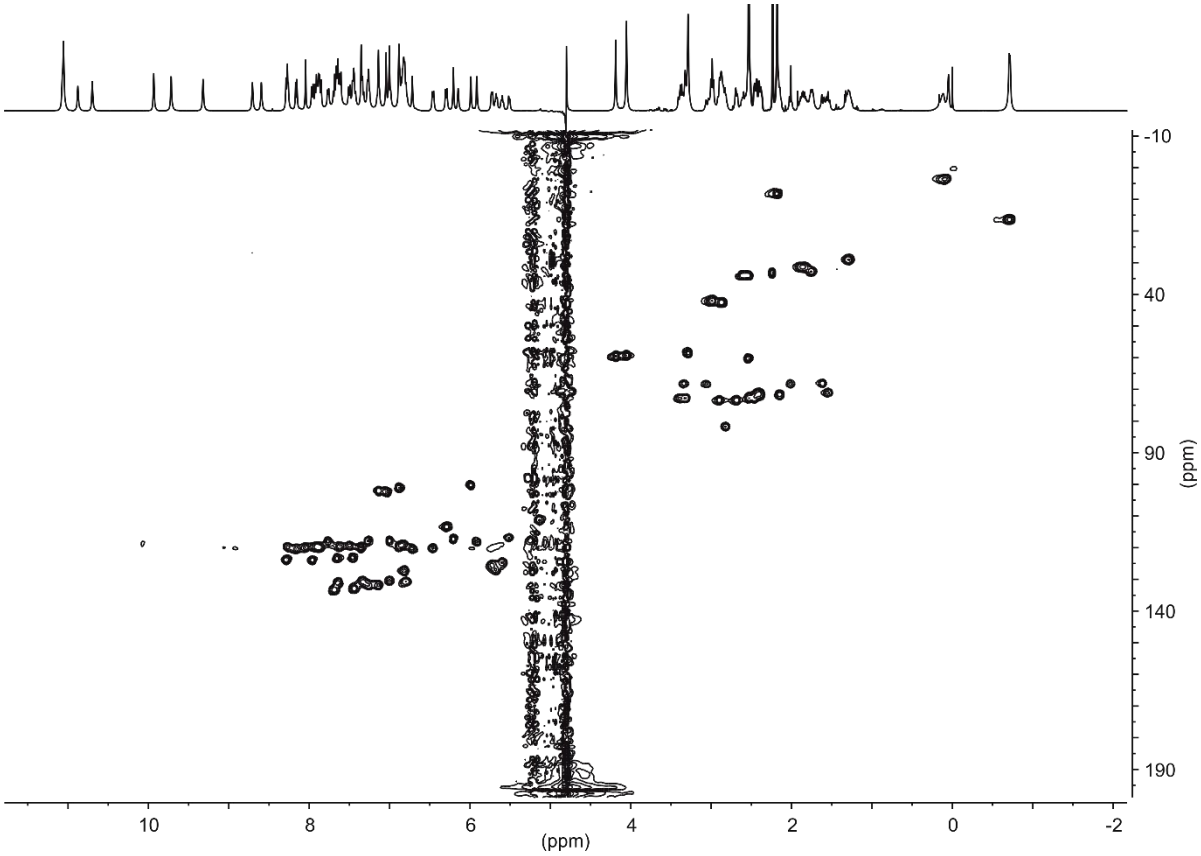

Figure S19. ^{1}H-^{13}C HSQC spectrum of **1** (500 MHz, 27 mM sodium phosphate aqueous buffer pH 7.).

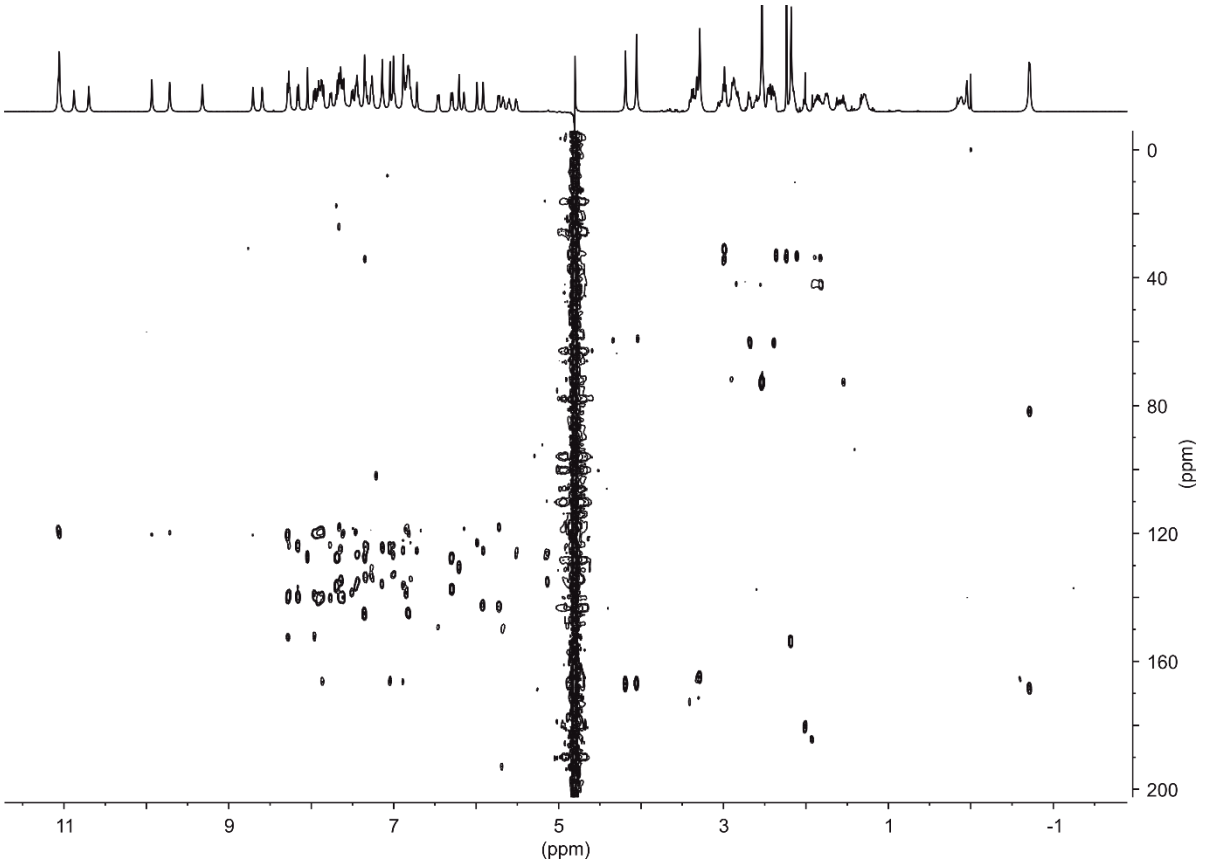

Figure S20. ^{1}H-^{13}C HMBC spectrum of **1** (500 MHz, 27 mM sodium phosphate aqueous buffer pH 7.0).

3.2 DOSY NMR of oligomers 1 and 2

The DOSY spectra were recorded on a Avance III HD 500 MHz Bruker BioSpin spectrometer equipped with a broad band observe 5-mm BB-H&FD CryProbe^{TM} Prodigy with a pulse sequence with stimulated echo using bipolar gradient pulses for diffusion and a 3-9-19 watergate solvent suppression pulse sequence from the Bruker pulse program library (stebpgp1s19). The diffusion delay Δ (big delta) was set to 175 ms and the diffusion gradient pulse length δ (little delta) was set to 1.1 ms. The number of gradient steps were set to 32 with linear spacing starting from 2% reaching 95% of the full gradient strength in the final step. For each of the 32 gradient amplitudes, 128 transients of 32k complex data points were acquired. DOSY processing was performed with the DOSY processing tool from MestReNova (v.12.0.0-20080) employing the Peak Heights Fit algorithm including the options "use existing peaks", "autocorrect peak positions", and "overlapped peaks analysis" with 32 points in diffusion dimension and a window of $1.00*10^{-4}$ to $1.00*10^{-8}$ cm^2 s^{-1}.

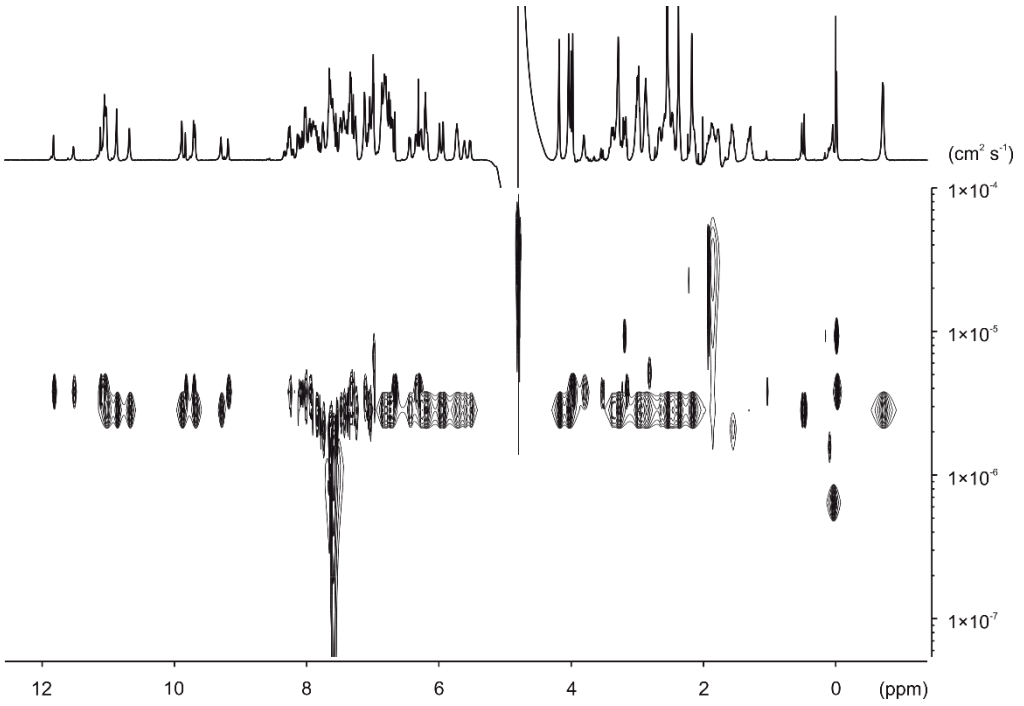

Figure S21. DOSY spectrum of a mixture of **1** (1 mM) and **2** (1 mM) in 27 mM sodium phosphate aqueous buffer pH 7.0.

4 X-ray Crystallography

After lyophilization, compound **1** was dissolved in pure water to a final concentration of 10 mM. Crystallization trials were performed at 20 °C by standard aqueous sitting drop vapor diffusion method and subsequently optimized by hanging drop vapor diffusion method at 20 °C. Hexagonal prisms (Figure S22) were obtained by mixing 0.5 µL of **1** and 0.5 µL of crystallization reagent comprising 20% w/v polyethylene glycol 8,000, 10 mM TRIS aqueous buffer, pH 7.5, 10 mM calcium chloride; equilibrated against 500 µL of crystallization reagent in the reservoir. For data collection, a single crystal was fished using a MiTeGen microloop, cryo-protected in a solution composed of 30% v/v polyethylene glycol 400 and 20% w/v polyethylene glycol 8,000 and flash frozen in liquid nitrogen.

Synchrotron data was collected on beam line P14 operated by EMBL Hamburg at the Petra III storage ring (DESY, Hamburg, Germany) using 0.9762 Å wavelength. During data collection, the crystal was cooled to 100 K. The crystal was exposed for 0.008 s and 0.2° oscillation per frame and a rotation pass of 360° was measured using an EIGER 16M detector. Data were processed using *autoPROC* pipeline.[7] The crystal belonged to the monoclinic space group $P2_1$ with unit cell parameters a = 21.400 (9) Å, b = 35.063 (1) Å, c = 23.820 (9) Å and β = 100.84 (4)°, V = 17,554 (10) Å^3 and two independent molecules in the asymmetric unit.

The structure was solved using dual space method with the program *SHELXD*[8] and refined by the full-matrix least-squares method on F^2 with *SHELXL*-2014[9] within *Olex2*.[10] After each refinement step, visual inspection of the model and the electron-density maps were carried out using *Olex2* and *Coot*.[11] AFIX, DFIX, EADP and FLAT instructions were used to improve the geometry of molecules and temperature parameters. One CH_3 group was severely disordered in one diethylene glycol tail and omitted. All non-H atoms were refined with anisotropic displacement parameters. Hydrogen atoms were placed at idealized positions. Restraints on anisotropic displacement parameters were implemented with DELU, SIMU, RIGU and ISOR instructions. In the final stage of refinement *SQUEEZE*[12] procedure from Platon suite was introduced to remove unmodeled electron density. Calculated total potential solvent accessible void volume and electron counts per unit cell were 7519.3 Å^3 and 2307, respectively.

Statistics of data collection and refinement are described in Table S1. The final cif file was checked using IUCr's checkcif algorithm. Due to large volume fractions of disordered solvent molecules, weak diffraction intensity and poor resolution, a number of A- and B-level remain in the checkcif file. These alerts are inherent to the data and refinement procedures and illustrate the limited practicality of the checkcif tool for medium- size molecule crystallography. They are listed below and have been divided into two groups. The first group illustrates weak quality of the data and refinement statistics if compared to that expected for small molecule structures from highly diffracting crystals. The second group is connected to decisions made during refinement and explained below. Atomic coordinates and structure

factors for $(\mathbf{1})_2$ was deposited in the Cambridge Crystallographic Data Centre (CCDC) with accession code 2122518. The data is available free of charge upon request (www.ccdc.cam.ac.uk/).

Group 1 alerts:

THETM01_ALERT_3_A The value of sine(theta_max)/wavelength is less than 0.550
Calculated sin(theta_max)/wavelength = 0.4673
PLAT029_ALERT_3_A _diffrn_measured_fraction_theta_full value Low . 0.915 Why?
PLAT341_ALERT_3_B Low Bond Precision on C-C Bonds 0.0197 Ang.
PLAT911_ALERT_3_B Missing FCF Refl Between Thmin & STh/L= 0.467
PLAT241_ALERT_2_B High 'MainMol' Ueq as Compared to Neighbors of
PLAT242_ALERT_2_B Low 'MainMol' Ueq as Compared to Neighbors of

Group 2 alerts:

SHFSU01_ALERT_2_A The absolute value of parameter shift to su ratio > 0.20
Absolute value of the parameter shift to su ratio given 2.141
Additional refinement cycles did not improve this.
PLAT080_ALERT_2_A Maximum Shift/Error 2.14 Why?
Additional refinement cycles did not improve this.
PLAT031_ALERT_4_A Refined Extinction Parameter within Range 0.000 Sigma
Extinction parameter was removed.

Table S3. Crystallographic data and refinement details for (**1**)$_2$.

Chemical formula	$C_{123.5}$ $H_{103.75}$ $N_{20.75}$ O_{34} S_3 Se_1
Formula weight	2597.66
Temperature	100 (2) K
Wavelength	0.9762 Å
Crystal system	Monoclinic
Space group	$P2_1$
Unit cell dimensions	a = 21.400 (9) Å, b = 35.063 (10) Å, c = 23.820 (9) Å α = 90°, β = 100.848 (4)°, γ = 90°
Volume	17554 (10) Å^3
Z	4
Density (calculated)	0.983 g/cm^3
Absorption coefficient	0.719 μ/mm^{-1}
Color and shape	Yellow, prism
Crystal size	0.05 x 0.05 x 0.18 mm
Index ranges	-19 ≤ h ≤ 19, -32 ≤ k ≤ 32, -22 ≤ l ≤22
Completeness to Θ = 27.14°	91.2 %
Reflections collected	91128
Independent reflections	27368 [R_{int} = 0.0745, R_{sigma} = 0.0655]
Data/restraints/parameters	27368/1066/2079
Goodness-of-fit on F^2	1.086
Final R indexes [$I > 2\sigma(I)$]	R_1 = 0.0899, wR_2 = 0.2555
Final R indexes [all data]	R_1 = 0.1235, wR_2 = 0.2950
Largest diff. peak and hole	0.57/-0.29 e Å^{-3}
CCDC #	2122518

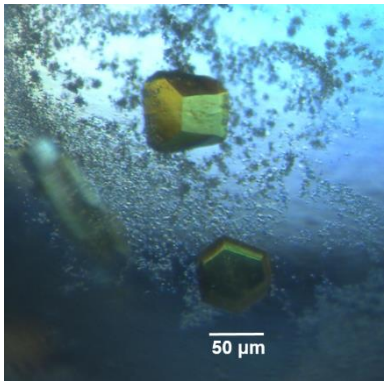

Figure S22. Crystals of (**1**)$_2$ observed under crossed polarizing microscope.

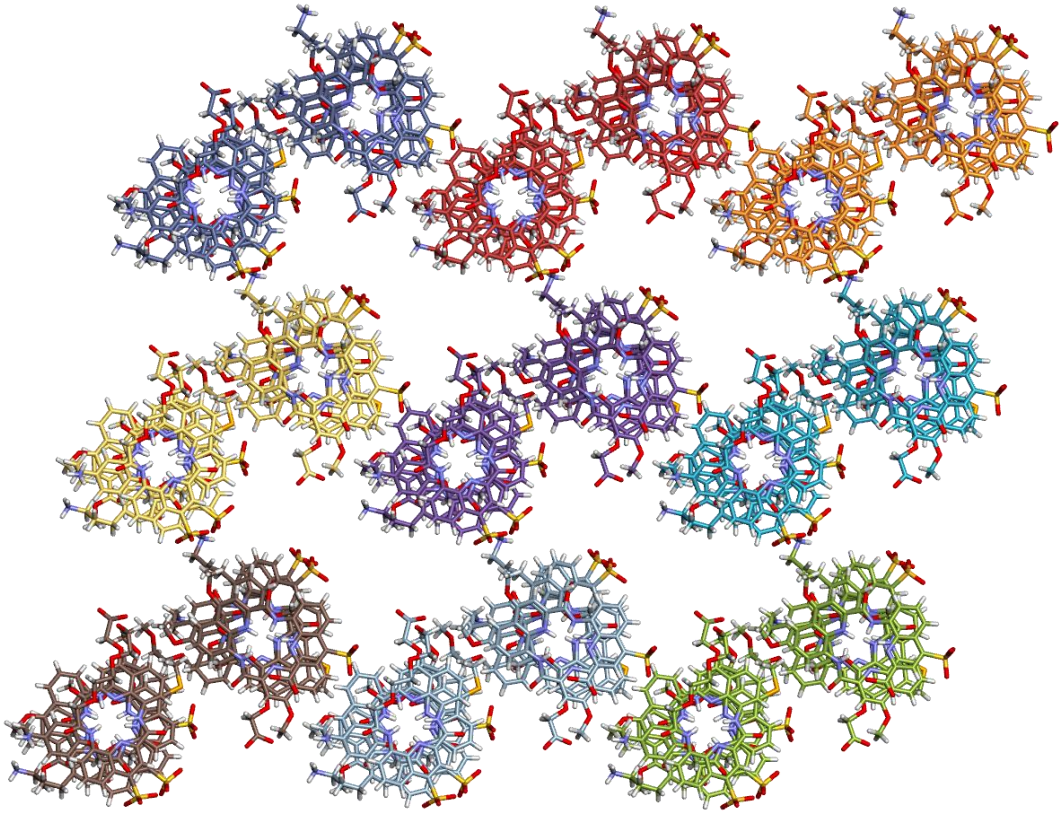

Figure S23. Packing of **1** in the crystal viewed down the b-axis. Helices in the same unit cell are shown in the same color.

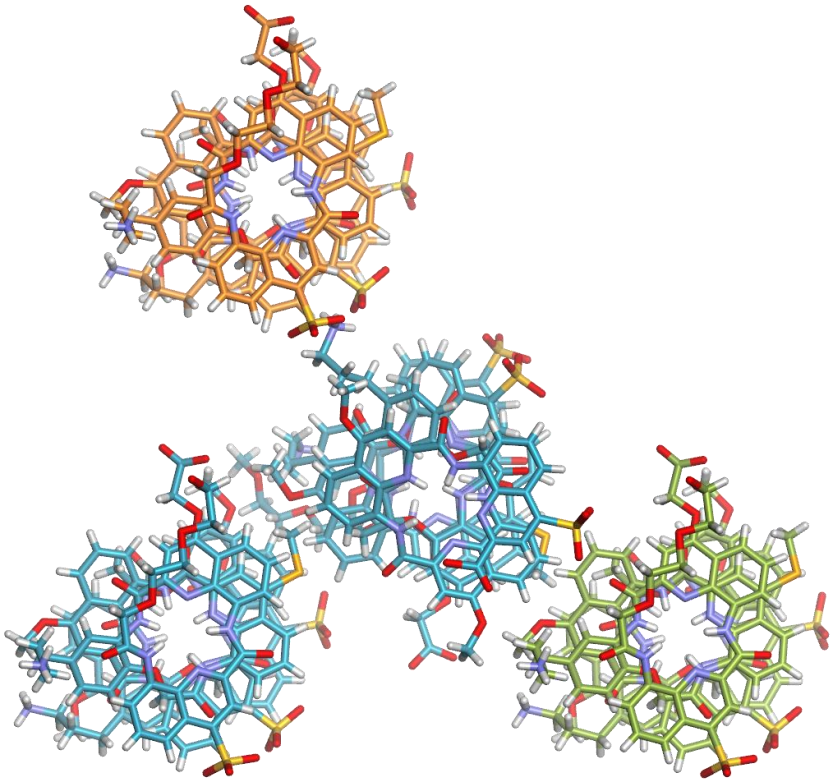

Figure S24. Coplanar neighbors in the crystal structure of **1**. Helices in the same unit cell are shown in the same color. Each helix (illustrated by the middle helix in this figure) has three different coplanar neighbors: two are mediated by hydrophobic contacts (blue and green neighbor), one is mediated by a salt bridge (orange neighbor).

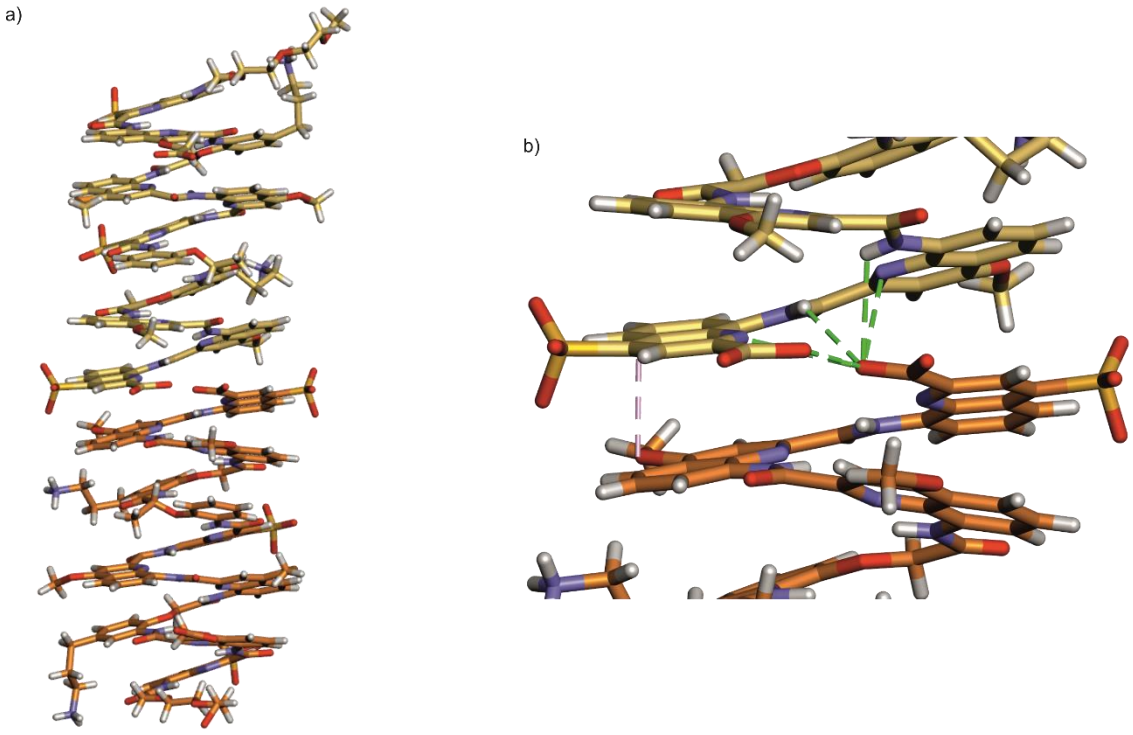

Figure S25. Stacking of helices via their C-termini in the crystal structure of **1** showing two whole helices (a) and a zoom on the intermolecular interface (b). Hydrogen bonding interactions and hydrophobic contacts are shown by green and pink dashed lines, respectively.

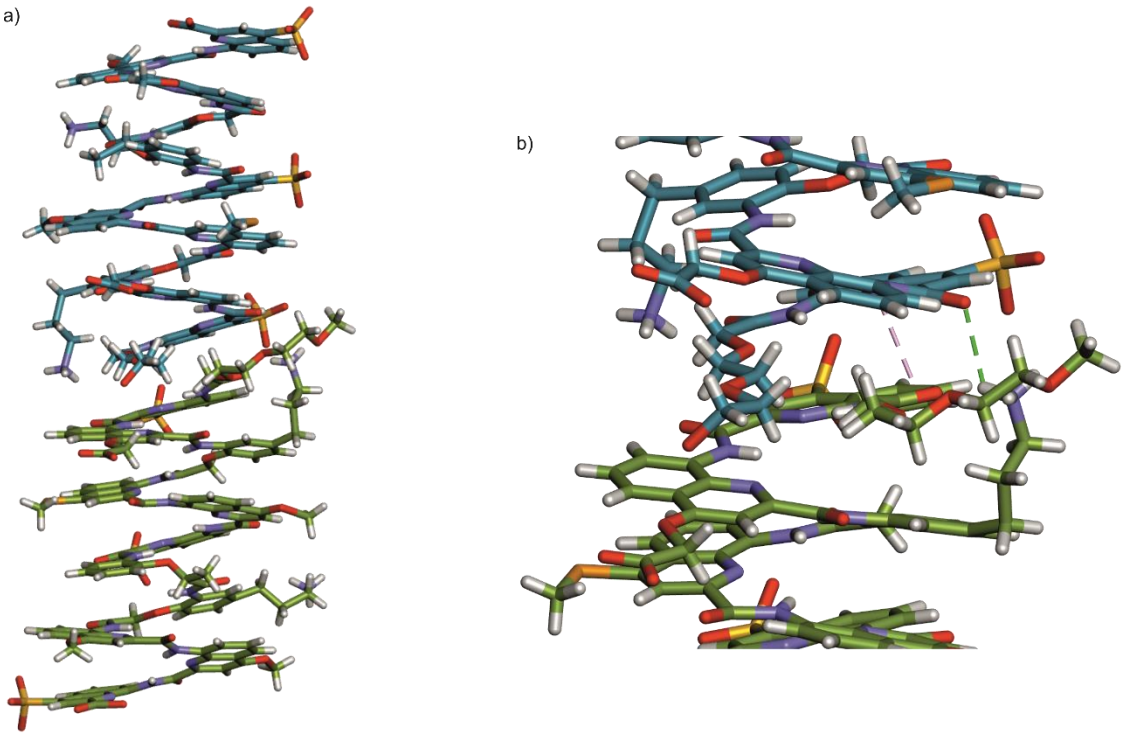

Figure S26. Stacking of helices via their N-termini in the crystal structure of **1** showing two whole helices (a) and a zoom on the intermolecular interface (b). Hydrogen bonding interactions and hydrophobic contacts are shown by green and pink dashed lines, respectively.

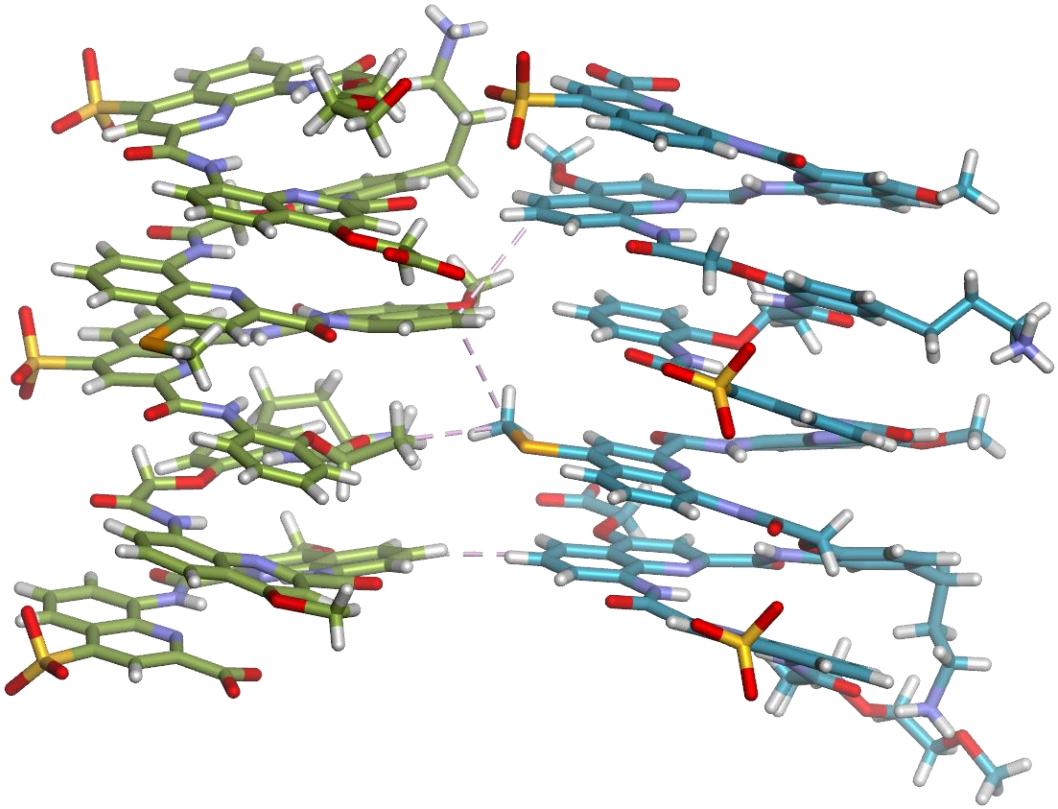

Figure S27. Tightest side-to-side helix-helix interface mediated by hydrophobic contacts in the crystal structure of **1**. Close hydrophobic contacts are highlighted by dashed lines.

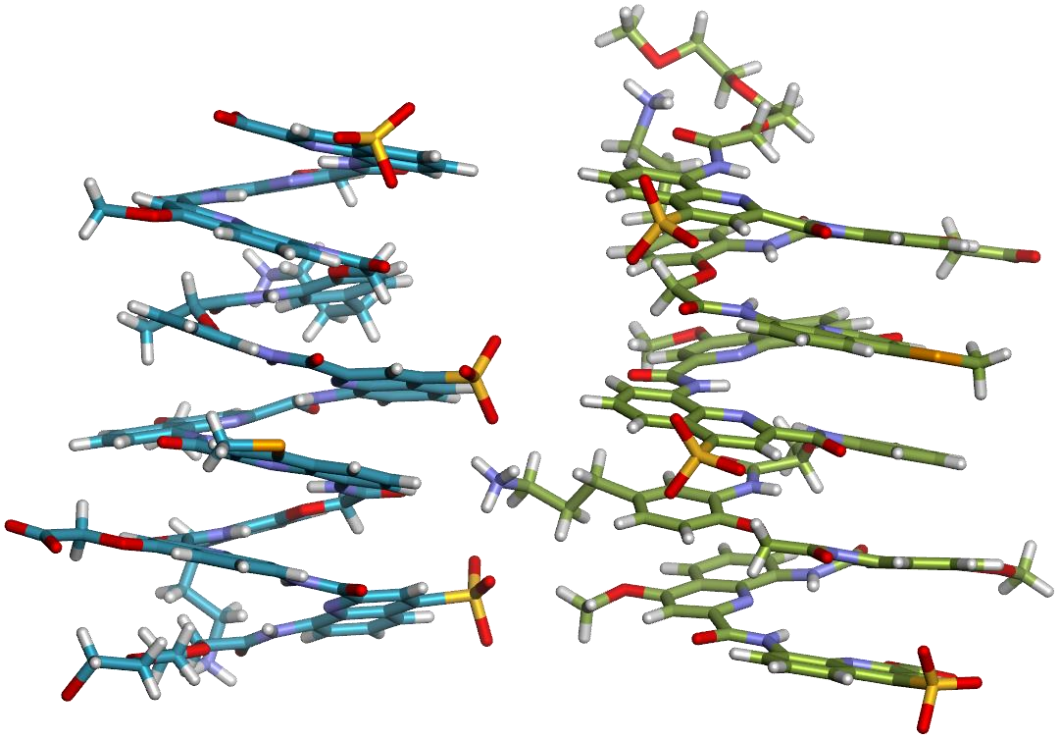

Figure S28. Intermolecular salt-bridge observed between the side chains of a B^{Orn} and two Q^{Sul} units in the crystal structure of **1**.

5 Spectra and chromatograms of new compounds

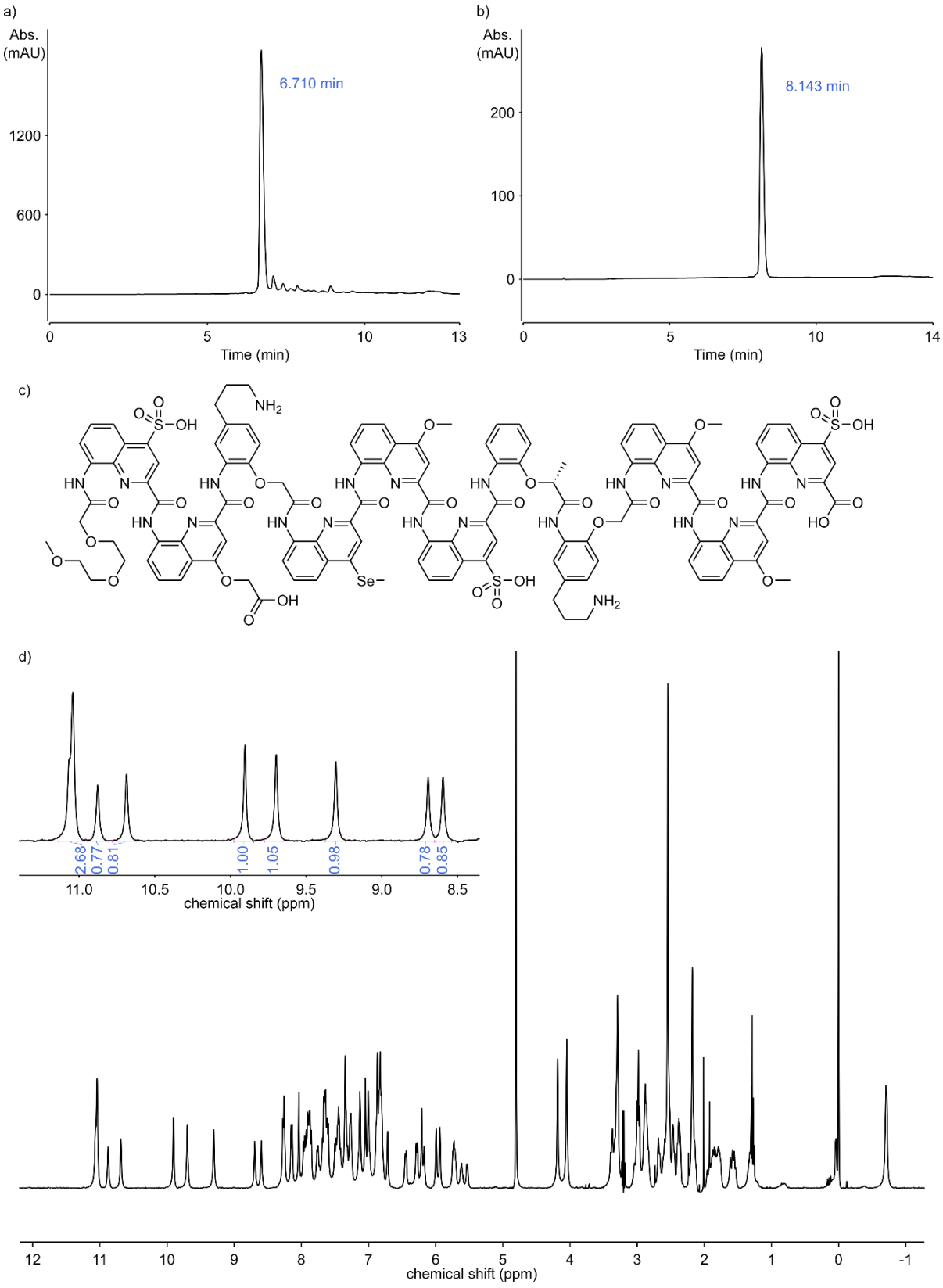

Figure S29. Analytical data of compound **1**. HPLC chromatograms after cleavage from the resin (a) and after purification (b) (C8, 0–40B, 50 °C; A: 13mM ammonium acetate aqueous buffer pH 8.5, B: acetonitrile). c) Chemical structure of compound **1**. d) ^{1}H NMR spectrum (500 MHz, 1.0 mM in 27 mM sodium phosphate aqueous buffer pH 7.0).

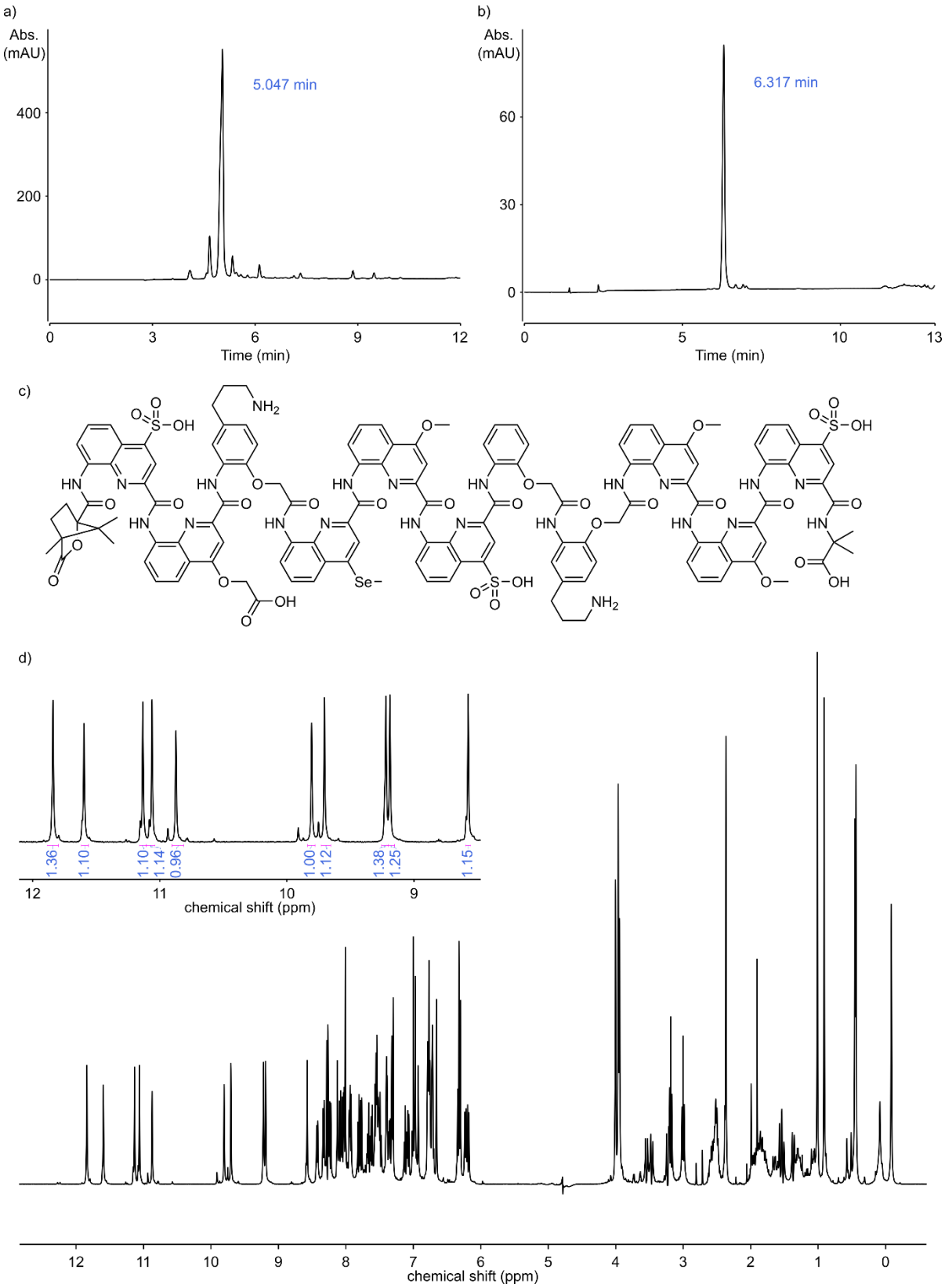

Figure S30. Analytical data of compound **2**. HPLC chromatograms after cleavage from the resin (a) (C8, 0–60B, 50 °C; A: 13mM ammonium acetate aqueous buffer pH 8.5, B: acetonitrile) and after purification (b) (C8, 0–35B, 50 °C; A: 13mM ammonium acetate aqueous buffer pH 8.5, B: acetonitrile). c) Chemical structure of compound **2**. d) ^{1}H NMR spectrum (500 MHz, 1.0 mM in H_2O/D_2O 9:1).

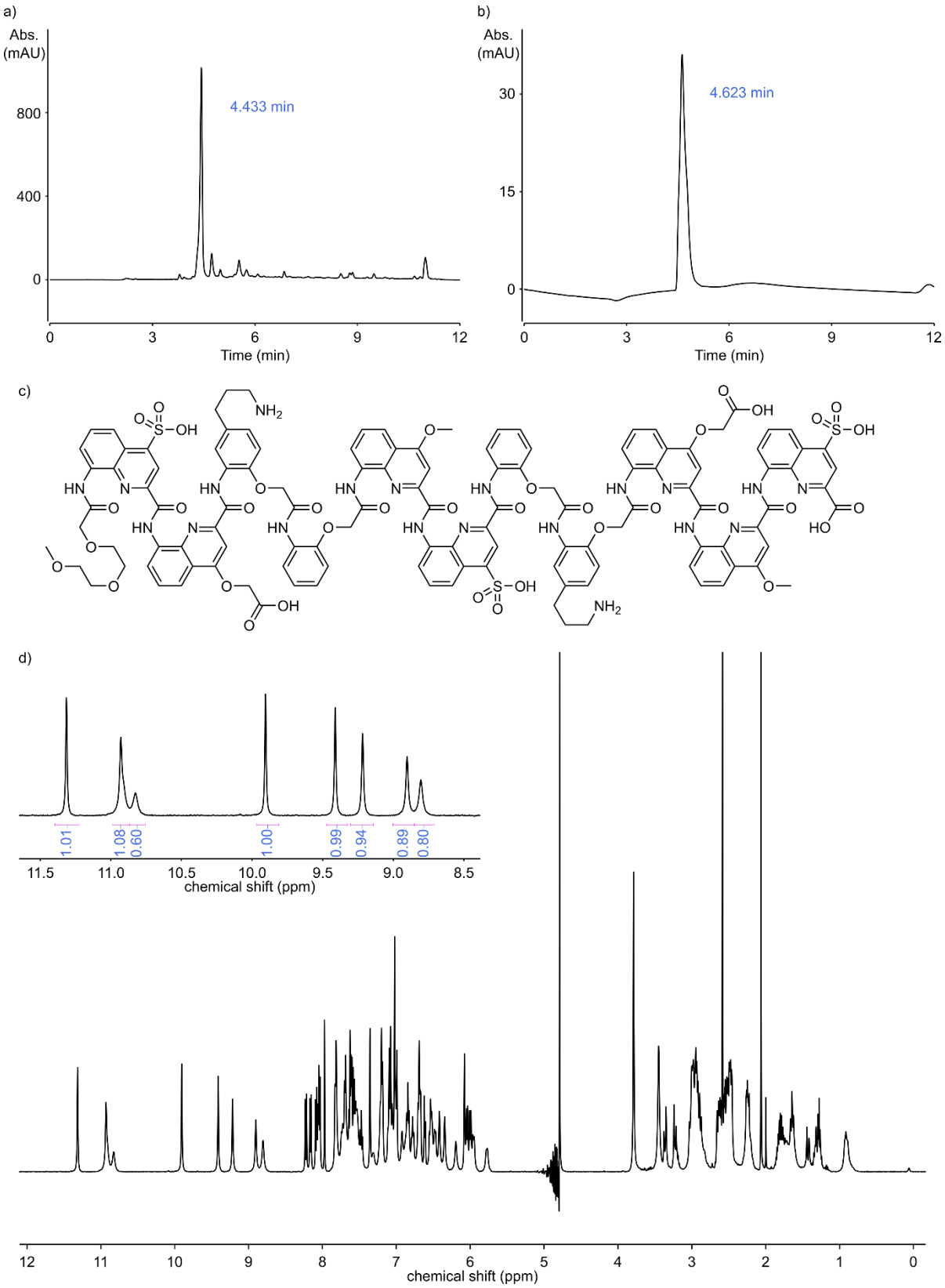

Figure S31. Analytical data of compound **3**. HPLC chromatograms after cleavage from the resin (a) (C8, 0–40B, 50 °C; A: 13mM ammonium acetate aqueous buffer pH 8.5, B: acetonitrile) and after purification (b) (C8, 0–60B, 25 °C; A: 13mM ammonium acetate aqueous buffer pH 8.5, B: acetonitrile). c) Chemical structure of compound **3**. d) ^{1}H NMR spectrum (500 MHz, 0.5 mM in H_2O/D_2O 9:1).

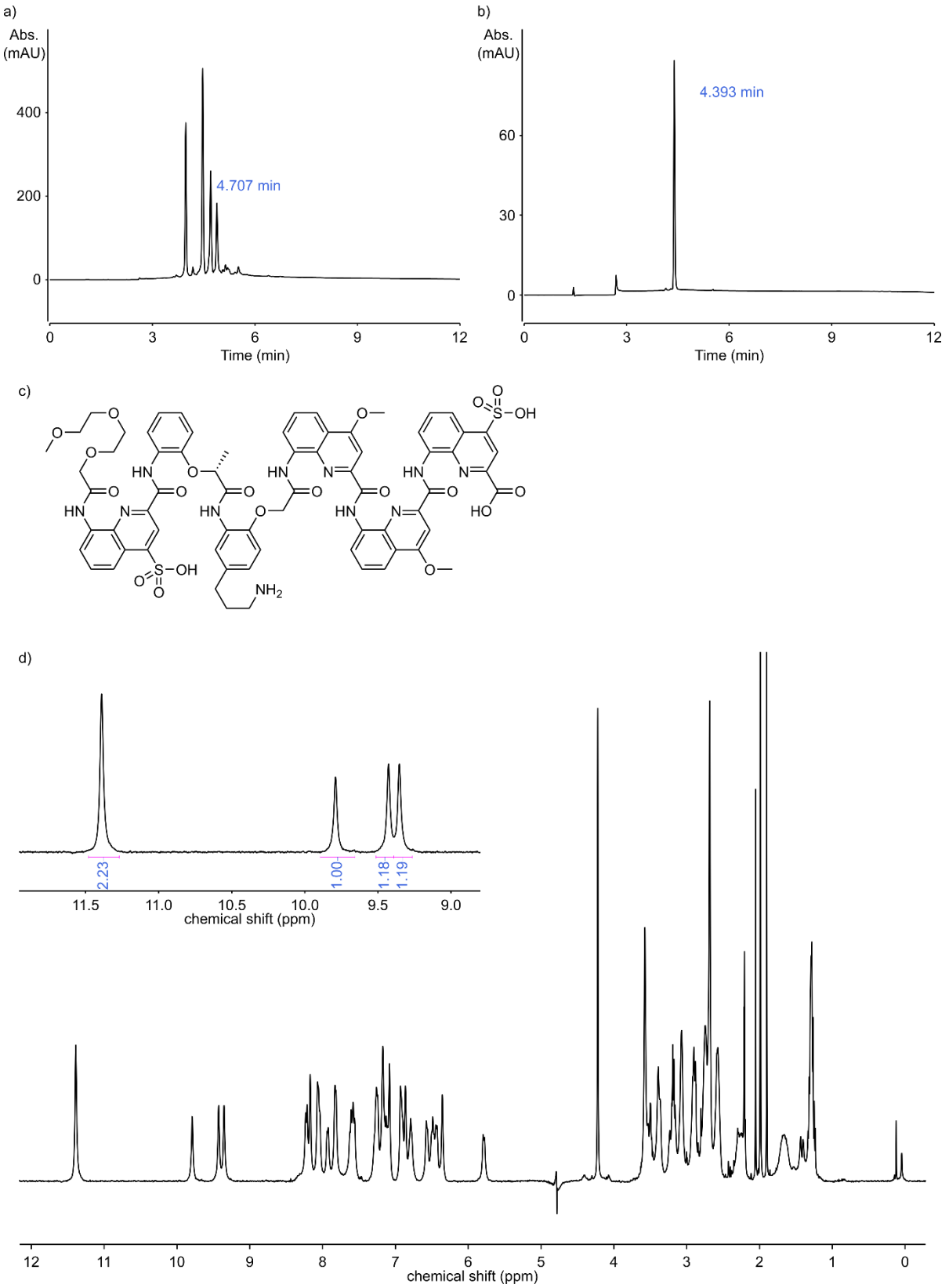

Figure S32. Analytical data of compound **4**. HPLC chromatograms after cleavage from the resin (a) and after purification (b) (C18, 0–100B, 50 °C; A: 13mM ammonium acetate aqueous buffer pH 8.5, B: acetonitrile). c) Chemical structure of compound **4**. d) ^{1}H NMR spectrum (500 MHz, 1.0 mM in 27 mM sodium phosphate aqueous buffer pH 7.0).

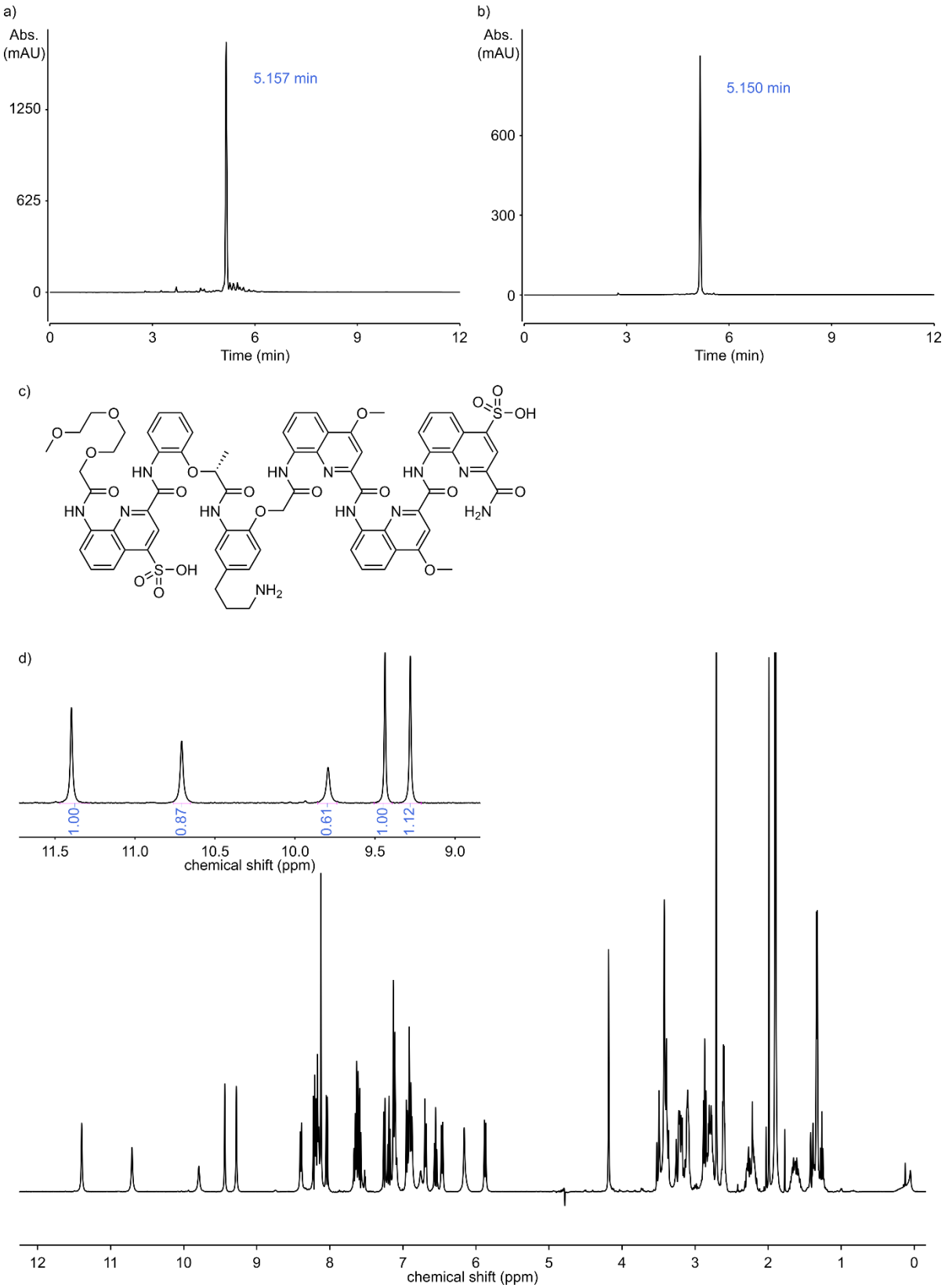

Figure S33. Analytical data of compound **5**. HPLC chromatograms after cleavage from the resin (a) and after purification (b) (C18, 0–100B, 50 °C; A: 13mM ammonium acetate aqueous buffer pH 8.5, B: acetonitrile). c) Chemical structure of compound **5**. d) ^{1}H NMR spectrum (500 MHz, 1.0 mM in 12 mM ammonium acetate aqueous buffer pH 7.0).

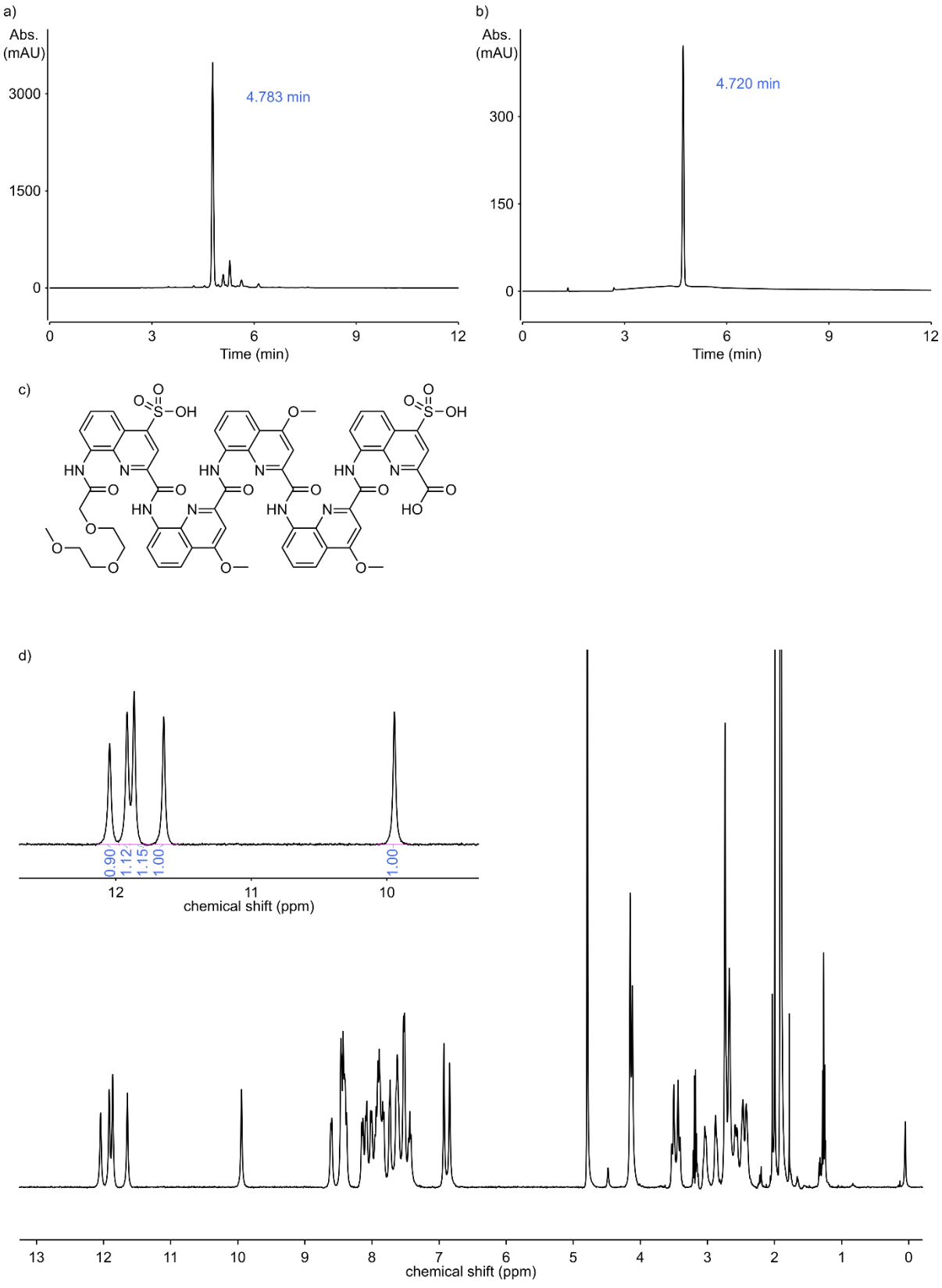

Figure S34. Analytical data of compound **6**. HPLC chromatograms after cleavage from the resin (a) and after purification (b) (C18, 0–100B, 50 °C; A: 13mM ammonium acetate aqueous buffer pH 8.5, B: acetonitrile). c) Chemical structure of compound **6**. d) ^{1}H NMR spectrum (500 MHz, 1.0 mM in 12 mM ammonium acetate aqueous buffer pH 7.0).

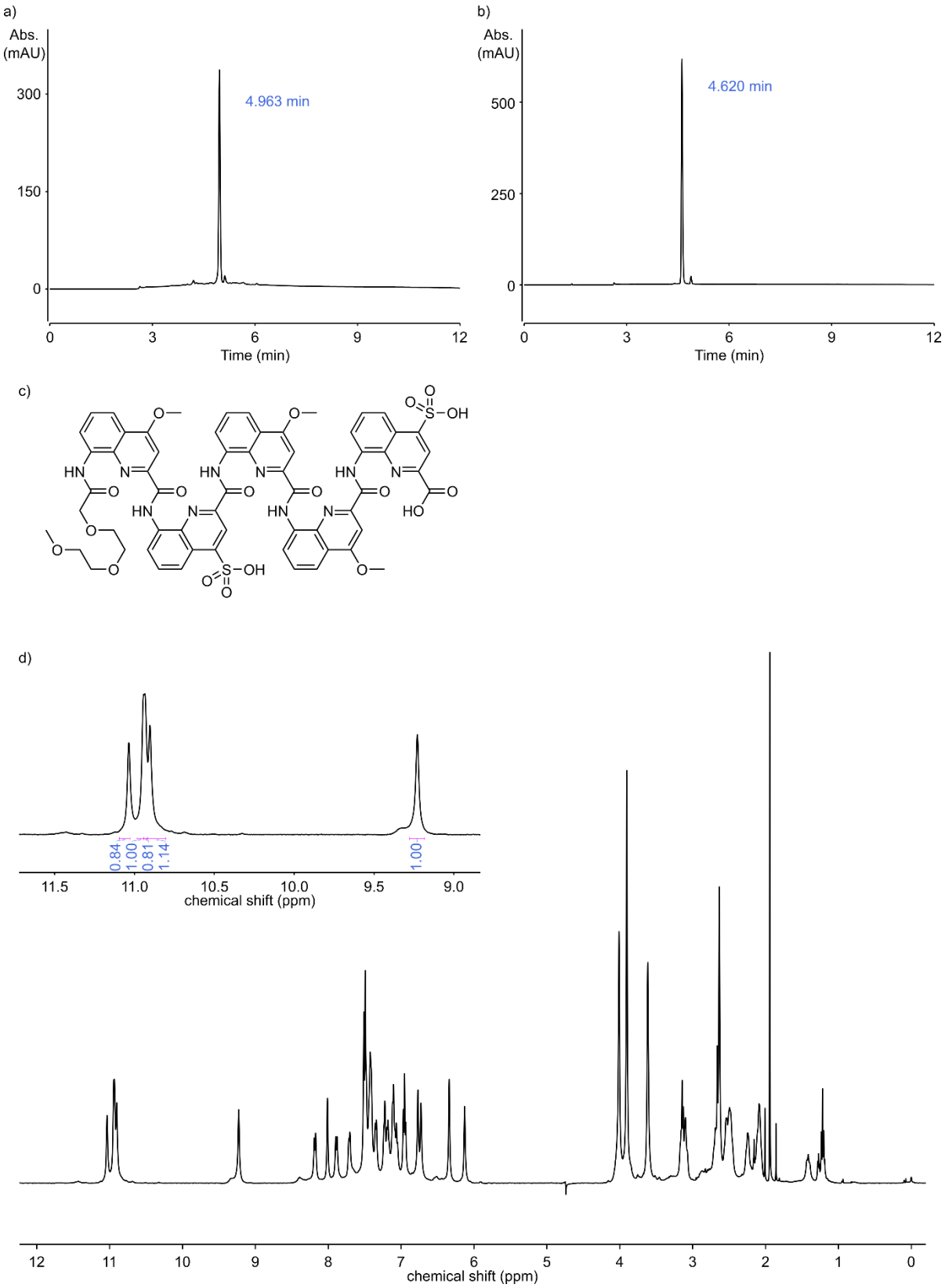

Figure S35. Analytical data of compound **7**. HPLC chromatograms after cleavage from the resin (a) and after purification (b) (C18, 0–30B, 50 °C; A: 13mM ammonium acetate aqueous buffer pH 8.5, B: acetonitrile). c) Chemical structure of compound **7**. d) ^{1}H NMR spectrum (500 MHz, 5.0 mM in 27 mM sodium phosphate aqueous buffer pH 7.0).

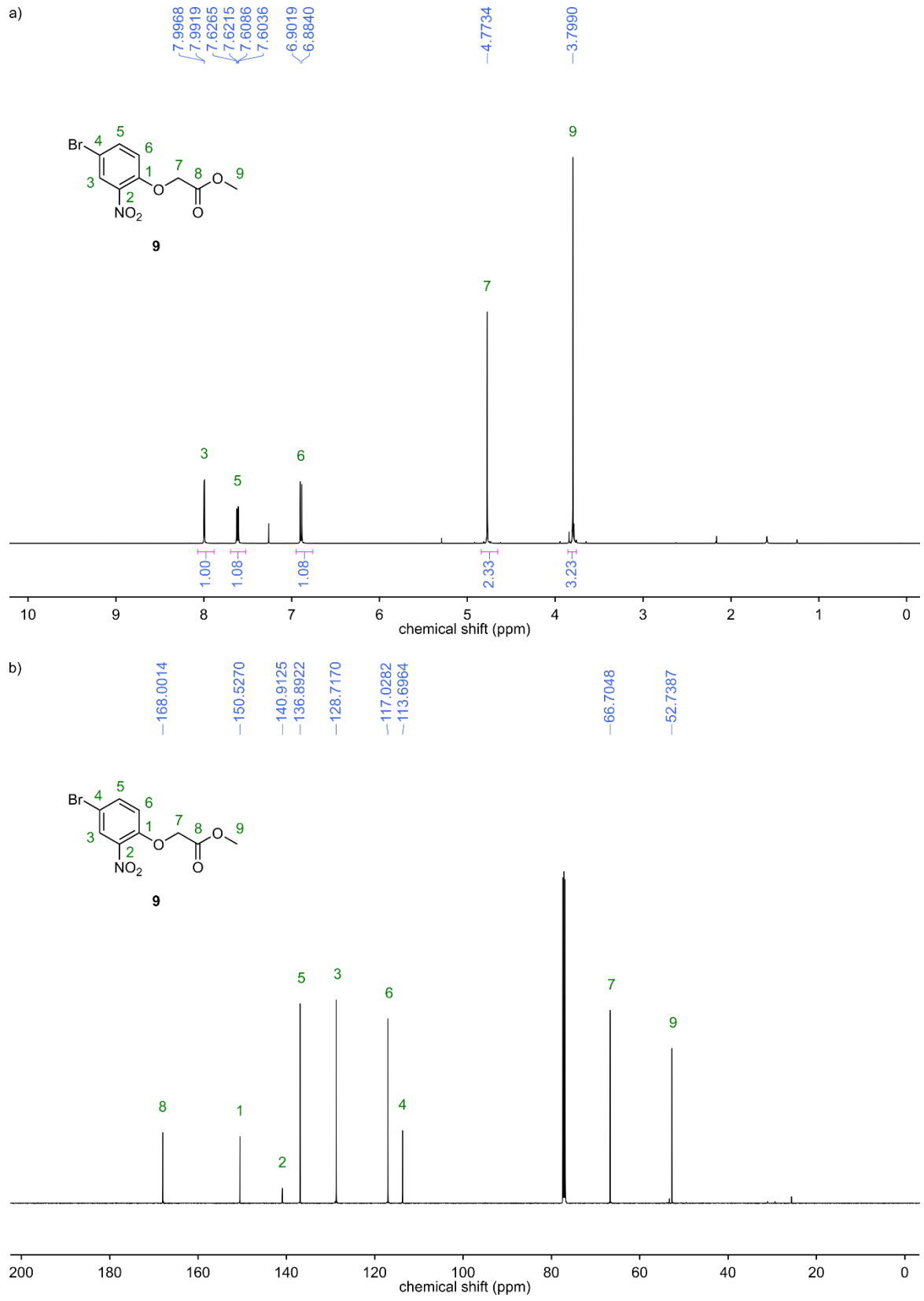

Figure S36. NMR spectra of compound **9**. a) ^{1}H NMR (500 MHz, $CDCl_3$). b) ^{13}C NMR (126 MHz, $CDCl_3$).

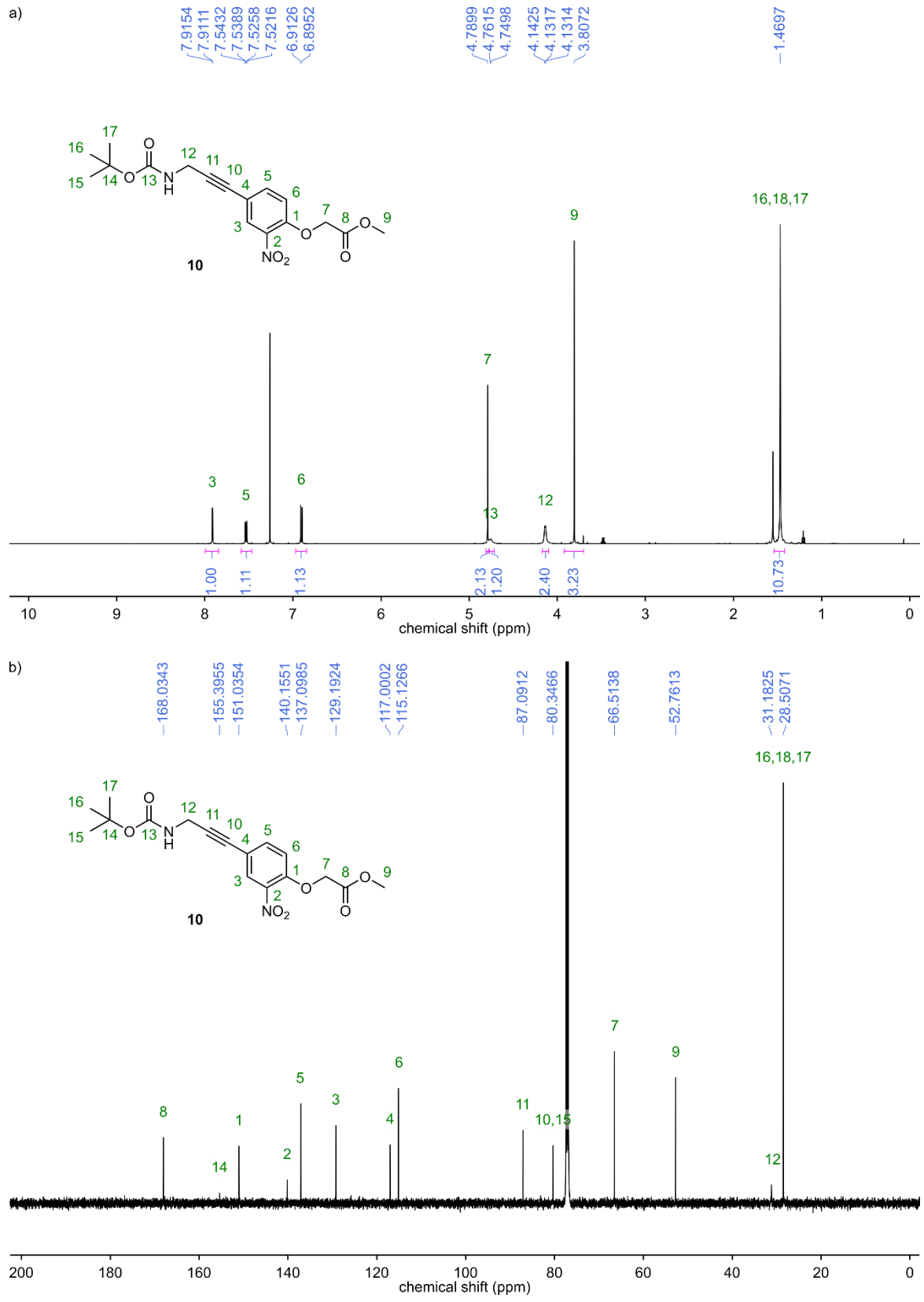

Figure S37. NMR spectra of compound **10**. a) ^{1}H NMR (500 MHz, $CDCl_3$). b) ^{13}C NMR (126 MHz, $CDCl_3$).

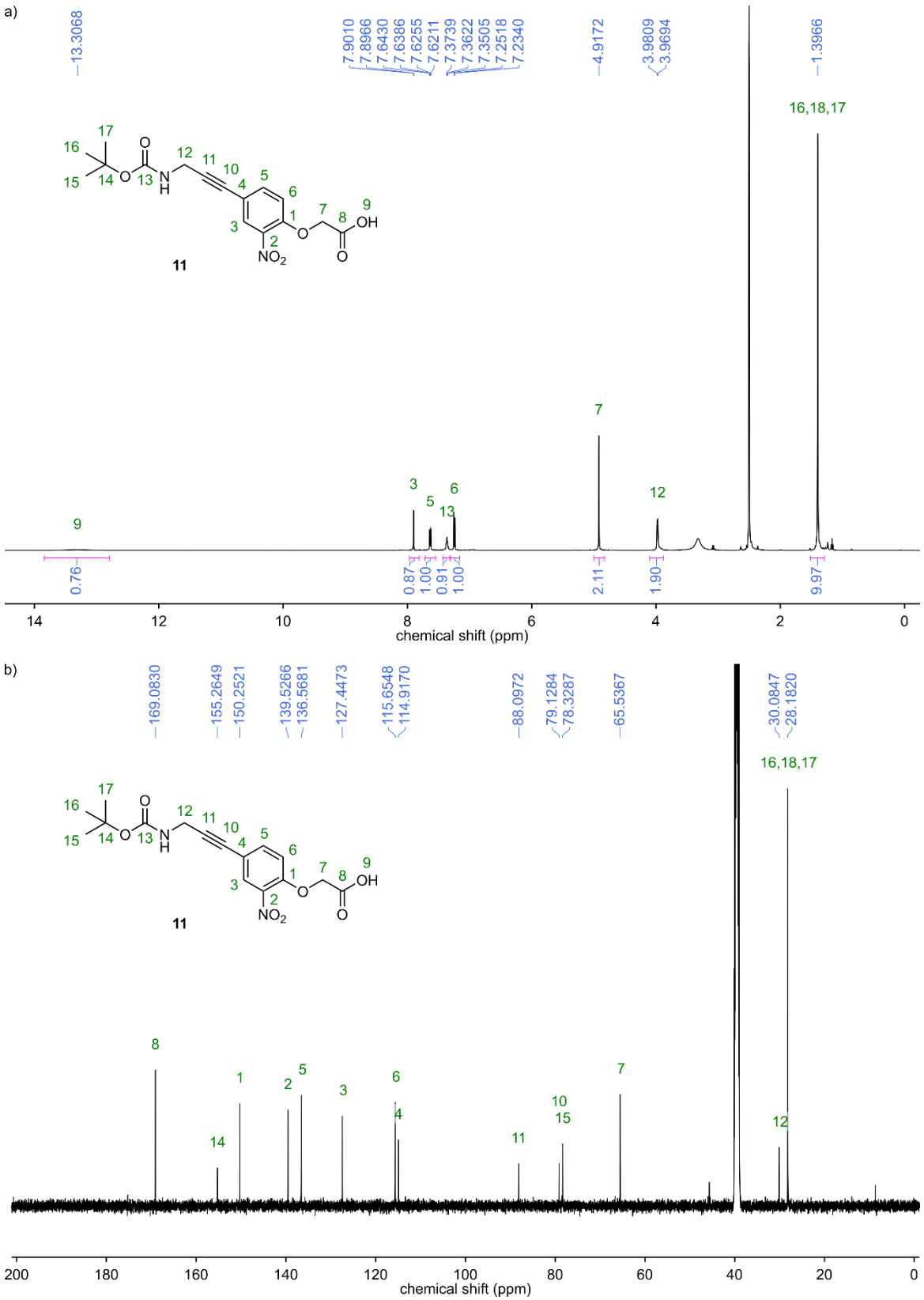

Figure S38. NMR spectra of compound **11**. a) ^{1}H NMR (500 MHz, DMSO-d_6). b) ^{13}C NMR (126 MHz, DMSO-d_6).

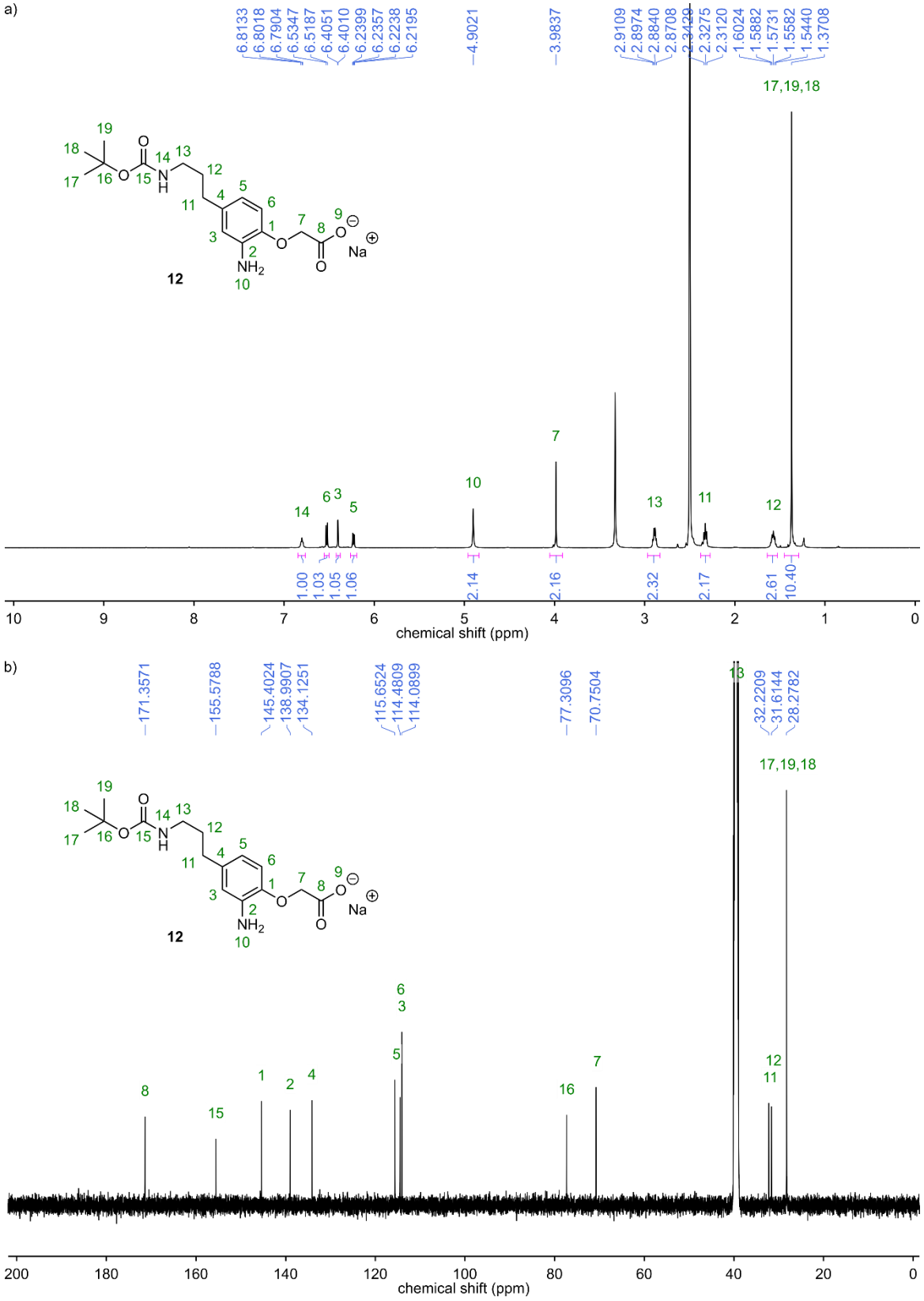

Figure S39. NMR spectra of compound **12**. a) ^{1}H NMR (500 MHz, DMSO-d_6). b) ^{13}C NMR (126 MHz, DMSO-d_6).

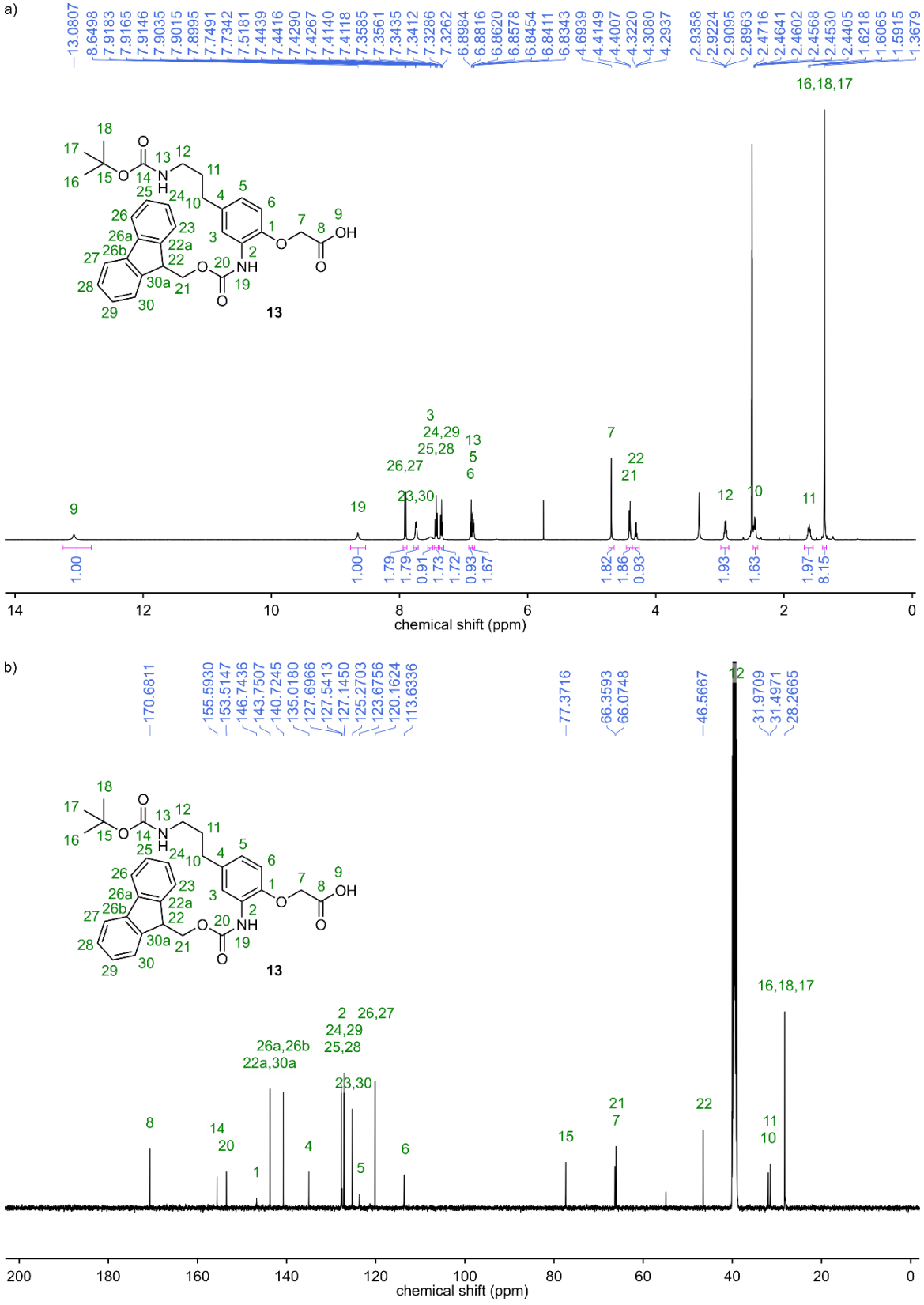

Figure S40. NMR spectra of compound **13**. a) ^{1}H NMR (500 MHz, DMSO-d_6). b) ^{13}C NMR (126 MHz, DMSO-d_6).

6 References

[1] X. Hu, S. J. Dawson, P. K. Mandal, X. De Hatten, B. Baptiste, I. Huc, *Chem. Sci.* **2017**, *8*, 3741-3749.

[2] B. t. Baptiste, C. l. Douat-Casassus, K. Laxmi-Reddy, F. d. r. Godde, I. Huc, *J. Org. Chem.* **2010**, *75*, 7175-7185.

[3] J. Buratto, C. Colombo, M. Stupfel, S. J. Dawson, C. Dolain, B. Langlois d'Estaintot, L. Fischer, T. Granier, M. Laguerre, B. Gallois, I. Huc, *Angew. Chem. Int. Ed.* **2014**, *53*, 883-887; *Angew. Chem.* **2014**, *126*, 902-906.

[4] D. Bindl, E. Heinemann, P. K. Mandal, I. Huc, *Chem. Commun.* **2021**, *57*, 5662–5665.

[5] a) H. E. Gottlieb, V. Kotlyar, A. Nudelman, *J. Org. Chem.* **1997**, *62*, 7512-7515; b) L. Pohl, M. Eckle, *Angew. Chem. Int. Ed.* **1969**, *8*, 381-381; *Angew. Chem.* **1969**, *81*, 395-395.

[6] X. Hu, S. J. Dawson, Y. Nagaoka, A. Tanatani, I. Huc, *J. Org. Chem.* **2016**, *81*, 1137-1150.

[7] a) P. Evans, *Acta Crystallogr. D* **2006**, *62*, 72-82; b) P. R. Evans, G. N. Murshudov, *Acta Crystallogr. D* **2013**, *69*, 1204-1214; c) W. Kabsch, *Acta Crystallogr. D* **2010**, *66*, 125-132; d) C. Vonrhein, C. Flensburg, P. Keller, A. Sharff, O. Smart, W. Paciorek, T. Womack, G. Bricogne, *Acta Crystallogr. D* **2011**, *67*, 293-302; e) M. D. Winn, C. C. Ballard, K. D. Cowtan, E. J. Dodson, P. Emsley, P. R. Evans, R. M. Keegan, E. B. Krissinel, A. G. W. Leslie, A. Mccoy, S. J. Mcnicholas, G. N. Murshudov, N. S. Pannu, E. A. Potterton, H. R. Powell, R. J. Read, A. Vagin, K. S. Wilson, *Acta Crystallogr. D* **2011**, *67*, 235-242.

[8] G. M. Sheldrick, *Acta Crystallogr. A* **2008**, *64*, 112-122.

[9] G. M. Sheldrick, *Acta Crystallogr. C* **2015**, *71*, 3-8.

[10] O. V. Dolomanov, L. J. Bourhis, R. J. Gildea, J. A. K. Howard, H. Puschmann, *J. Appl. Cryst.* **2009**, *42*, 339-341.

[11] P. Emsley, B. Lohkamp, W. G. Scott, K. Cowtan, *Acta Crystallogr. D* **2010**, *66*, 486-501.

[12] A. L. Spek, *Acta Crystallogr. D* **2009**, *65*, 148-155.